参赛学生姓名：刘佳宸,金恩盛

中学：西安汉诺威国际学校

省份：陕西

国家/地区：中国大陆[刘佳宸],大韩民国[金恩盛]

指导老师1 姓名：German Camilo Quinonez

指导老师1 单位：汉诺威国际学校

论文题目：柠檬酸交联致密化木作为可降解骨固定材料的制备、力学性能与体外降解研究

Densified Juniper Wood Crosslinked with Citric Acid as a Candidate for Bone Fracture Fixation

Abstract:

Internal fixation plates made from stainless steel, titanium and cobalt-chromium are four to fifteen times stiffer than cortical bone. They shield bone from load and leave it weaker after union, obscure the fracture on radiographs, and do not resorb, so a second operation is usually needed to remove them. Densified wood (DW) is an appealing alternative, being renewable, radiolucent and of bone-like stiffness, but it swells and loses most of its stiffness in water and sheds almost no material into aqueous media. Both barriers share one cause: the fibril interfaces formed during pressing are held by hydrogen bonds, which water readily breaks, while the glycosidic backbone is scarcely attacked at all.

This work tested whether replacing part of that interface with covalent yet hydrolysable ester crosslinks could address both. Partially delignified juniper was impregnated with 10 wt% citric acid and cured at 170 °C before hot pressing, so that esterification occurred while the cell wall was still open and the modification reached the bulk rather than the surface. Ester formation was confirmed by an infrared carbonyl band at 1715 to 1745 cm^{-1} absent from the uncrosslinked control, with matched lignin-to-cellulose ratios establishing crosslinking as the only variable between the groups. Volume swelling fell by 28.2% and water uptake by 29.4%; stiffness retained after saturation rose 2.4-fold and retained flexural strength from 12.6% to 21.8%; and cellulose released into simulated body fluid over ten days, quantified by enzymatic hydrolysis followed by a dinitrosalicylic acid assay, rose by 49.6%. Retention of every mechanical property correlated positively with ester crosslink density.

That water uptake fell while cellulose release rose is the central finding, since it shows that swelling is governed by free hydroxyl groups and degradation by hydrolysable linkages, so the two can be adjusted independently rather than traded against one another. The improvements are real but insufficient for implant use: saturated stiffness remains near 1 GPa against the 15 to 25 GPa of cortical bone, dry flexural strength fell by 36.9% through reduced densification, and resorption is unproven because humans secrete no cellulase. The contribution is therefore the crosslinking chemistry itself, applied for the first time to a bulk lignocellulosic solid rather

than to isolated cellulose, together with a quantified account of what it achieves and where it stops.

Keywords: citric acid crosslinking; densified wood; ester crosslink; delignification; swelling resistance; cellulose release; wood modification

摘要

不锈钢、钛合金与钴铬合金制成的骨折内固定板，其刚度约为皮质骨的四至十五倍，会产生应力遮挡效应，使骨组织在愈合后反而变弱；同时在 X 射线影像中遮挡骨折部位，且不可降解，通常需经二次手术取出。密实化木材（densified wood, DW）可再生、对 X 射线透明，且刚度与皮质骨相近，因而成为具有潜力的替代材料；但其在水中会发生显著溶胀并损失大部分刚度，同时在水溶液中几乎不释放任何物质。这两项障碍源于同一原因：热压过程中形成的纤维界面依靠氢键维系，而氢键易被水破坏，纤维素主链的糖苷键却几乎不受侵蚀。

本研究考察以共价但可水解的酯交联取代部分氢键界面，能否同时改善上述两项性能。将部分脱木质素的杜松木以 10 wt%柠檬酸浸渍，并于热压前在 170 ℃下固化，使酯化反应在细胞壁仍处于开放状态时发生，从而使改性作用深入材料本体而非仅限于表面。红外光谱在 1715～1745 cm^{-1}处出现酯羰基特征吸收峰，而未交联对照组中并不存在该峰；两组木质素与纤维素峰面积比相当，证实交联是两组间唯一的变量。结果表明：体积溶胀率下降 28.2%，吸水率下降 29.4%；饱水后刚度保持率提高 2.4 倍，抗弯强度保持率由 12.6%升至 21.8%；经纤维素酶水解与 3,5-二硝基水杨酸法测定，十天内释放至模拟体液中的纤维素量增加 49.6%。各项力学性能的保持率均与酯交联密度呈正相关。

吸水量下降而纤维素释放量上升，是本研究的核心发现：溶胀由游离羟基的数量决定，降解则取决于可水解键的数量，二者可独立调控而非相互制约。改性效果确实存在，但尚不足以支撑植入应用：饱水状态下的模量仍仅约 1 GPa，远低于皮质骨的 15～25 GPa；干态抗弯强度因密实化程度下降而降低 36.9%；且由于人体不分泌纤维素酶，材料在体内的吸收降解亦未获证实。因此，本研究的贡献在于首次将柠檬酸酯交联应用于块体木质纤维素固体，而非以往的分离纤维素体系，并定量阐明了该方法的作用范围及其局限。

关键词： 柠檬酸交联；密实化木材；酯交联；脱木质素；抗溶胀；纤维素释放；木材改性

Catalogue

1. Introduction 11

1.1 Limitations of metallic fixation bone plates 8

1.2 Densified wood as a starting material 9

1.3 Remaining barriers after densification 11

1.4 Aim, research questions and original contribution 11

2. Theoretical Framework and Hypothesis 17

2.1 Ester crosslinking and reduced water uptake 13

2.2 Interfacial energy analysis 15

2.3 Ester links as a path for degradation 17

3. Methodology 26

3.1 Preparation 20

3.2 Chemical treatment 22

3.3 Hot pressing 23

3.4 Experimental design and specimen groups 24

3.5 Characterisation 26

4. Results 40

4.1 Evidence of ester formation 29

4.2 Densification change 30

4.3 Swelling and dimensional change 30

4.4 Mechanical properties and swelling retention 34

4.5 Degradability of densified wood 36

4.6 Impact of lignin and citric acid content.....38

4.7 Comparison with bone and established implant alloys 38

4.8 Measurement uncertainty 39

4.9 Summary of the effect of crosslinking 40

5. Conclusions 41

6. Discussion 45

6.1 Mechanical performance: what was achieved and what was not 43

6.2 Degradability: what was achieved and what was not 44

6.3 Materials-science contribution 44
6.4 Recommended further investigation 45
7. References 48
8. Appendix 49

1. Introduction

1.1 Limitations of metallic fixation bone plates

When a long bone fractures so badly that a cast will not hold the fragments in place, the standard treatment is open reduction and internal fixation (ORIF), in which a plate is screwed directly onto the bone so that the fragments stay aligned while the body heals them. Internal fixation does not heal the bone itself; it simply holds the geometry steady and carries load while natural remodelling takes place [8]. Almost all of these plates are metallic. Low-carbon 316L stainless steel is used for its strength, fatigue resistance and low cost; titanium alloy, usually Ti-6Al-4V, is used for its biocompatibility, corrosion resistance and better behaviour in magnetic resonance imaging; and cobalt-chromium alloys are used where very high strength is needed. All three have been implanted successfully in millions of patients [8]. Their limitations, however, are well recognised, and they fall into three groups.

The first is stiffness mismatch. The Young's modulus of human cortical bone is usually quoted as 15 to 25 GPa, with reported values from about 7 to 30 GPa depending on age, anatomical site, and measurement method [1]. Titanium alloy is about 110 GPa, stainless steel 190 to 200 GPa and cobalt-chromium 220 to 250 GPa, so a fixation plate is between four and fifteen times stiffer than the bone it is bolted to. When two elastic bodies are rigidly joined and loaded in parallel, the stiffer one carries the larger share of the load. The plate therefore takes most of the force healing bone would otherwise experience. This matters because bone is not an inert scaffold but a living tissue that remodels according to the mechanical demand placed on it, which is a principle known as Wolff's law (Figure 1). Where loading falls, resorption outpaces deposition, and bone mineral density around the implant declines. This effect, called stress shielding, weakens exactly the region the surgeon is trying to repair and raises the risk of refracture once the plate is removed.

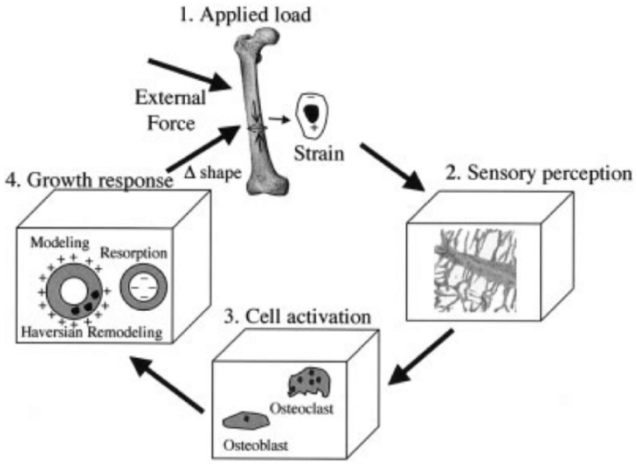


Figure 1: Response of bone to loading. Bone remodels in response to the mechanical loading it experiences, so a reduction in load leads to loss of bone density (respire physical therapy, 2023).

The second limitation is interference with medical imaging. Fracture healing is monitored by radiography and, where more detail is needed, by computed tomography. Metals are far denser than soft tissue or bone and absorb X-rays strongly, so an implant appears as a solid white mass and generates bright streak and dark band artefacts around itself (Figure 2). These artefacts are worst at the implant–bone interface, which is precisely the region a surgeon needs to inspect in order to judge whether union is progressing or whether delayed union or infection has developed [2]. The growing clinical use of radiolucent carbon-fibre-reinforced implants shows how much value is placed on being able to see through the hardware [3]. Cellulose, by contrast, is a low-density polymer built almost entirely from carbon, hydrogen and oxygen, so a wood-derived plate would be expected to be largely radiolucent.

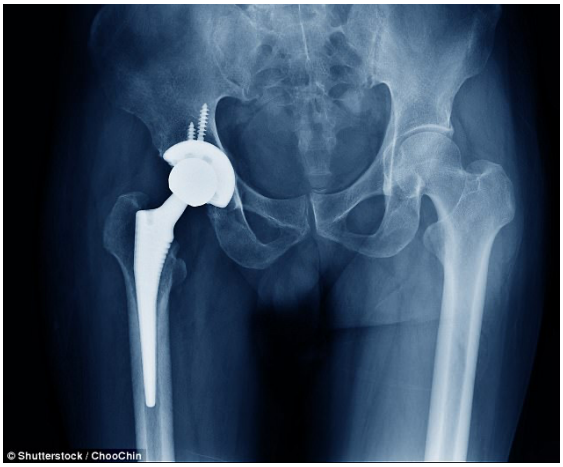


Figure 2*: Radiograph of a metallic orthopaedic implant. The metal is completely radio-opaque and obscures the bone immediately surrounding it (Shutterstock/ChooChin).*

The third limitation is permanence. Steel and titanium do not resorb, so once union is complete the plate has no further function but remains in the body. In younger patients it is commonly removed in a second operation, exposing the patient to another anaesthetic, another wound, another recovery period

and further cost. If it is left in place, slow bio-corrosion in the aggressive ionic environment of the body releases metal ions; 316L stainless steel for example contains 13 to 15 percent nickel, a recognised sensitiser, and the work of Rabin [4] notes that sensitivity reactions and late loosening are both documented consequences.

Taken together these three limitations define the specification that any replacement material has to meet: a stiffness close to that of bone rather than far above it, transparency to imaging, enough strength to carry bending loads during healing, and the ability to resorb afterwards.

1.2 Densified wood as a starting material

The starting point for this project is the densification process reported by Song and colleagues in Nature in 2018, which converts ordinary bulk wood into a dense, high-strength solid [6]. In the first step the wood is partially delignified by boiling it in aqueous NaOH and Na_2SO_3, which removes much of the lignin and hemicellulose that bind the cell walls together while leaving the crystalline cellulose framework largely intact. In the second step the softened, porous block is hot-pressed at about 100 °C under 5 MPa, causing the hollow cell lumens to collapse and pressing the cellulose fibrils into a dense and compacted sample.

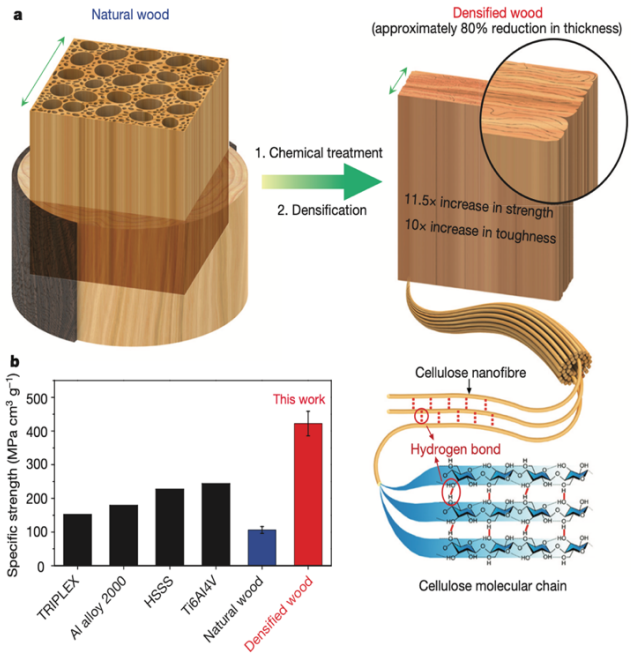


Figure 3: *The densification route and its effect on specific strength. (a) Chemical treatment followed by compression collapses the cellular structure and reduces the thickness by roughly 80%, bringing the cellulose nanofibres into intimate contact. (b) The specific strength of densified wood exceeds that of common structural alloys, including Ti-6Al-4V [6].*

That improved strength by the wood is interfacial. Removing lignin and hemicellulose allows the cell walls to collapse, and compression then brings the exposed cellulose fibril surfaces into contact at a separation short enough for extensive hydrogen bonding between their hydroxyl groups (Figure 4). Load is transferred between neighbouring chains through that hydrogen-bonded interface, so the number and density of these bonds, rather than the strength of the cellulose chains themselves, are the source of strength.

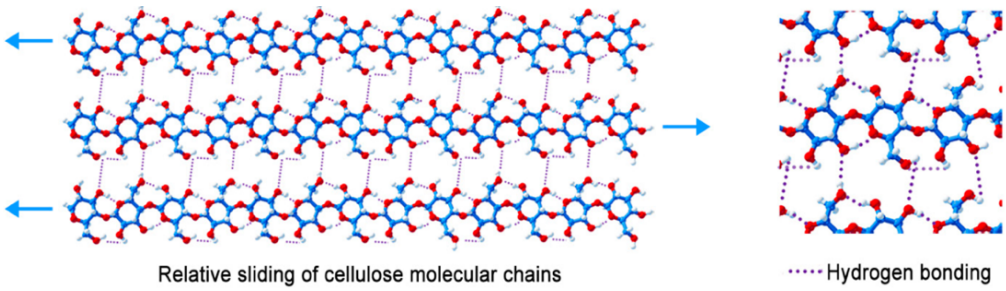


Figure 4: *Hydrogen bonding between adjacent cellulose molecular chains. Because these interchain bonds carry the load between fibrils, relative sliding of the chains is resisted by the hydrogen-bond network rather than by covalent bonding [6].*

1.3 Remaining barriers after densification

Ordinary densified wood is extremely venerable to swelling. Andze and colleagues [8] immersed specimens in boiling saline for two hours and measured the dimensional change; their results are reproduced in Table 1. Untreated juniper swelled by 13% in volume and dry-densified wood by 22%, but wet-densified wood, which is the route that gives the best dry mechanical properties, swelled by 52% and recovered essentially the whole of the compression that had been applied to it. Longitudinal swelling was negligible at around 0.1%, while radial swelling, measured along the axis in which the material had been compressed, reached 49 to 67%, showing how the material swells moving back towards the shape it had before pressing.

Swelling	Untreated	DD	WD	K0	K10	K20	K40
Volume (%)	13 ± 6	22 ± 6	52 ± 3	34 ± 8	32 ± 4	44 ± 2	38 ± 4
Longitudinal (%)	0.08	0.11	0.13	0.09	0.2	0.10	0.17
Tangential (%)	5.5	4.0	4.9	4.1	4.8	3.7	4.0
Radial (%)	20 ± 3	34 ± 5	67 ± 4	49 ± 5	57 ± 5	52 ± 2	60 ± 4

Table 1: *Volumetric and directional swelling of untreated and densified juniper wood after two hours in boiling saline. K0 to K40 denote Kraft cooking times of 0 to 40 minutes; DD and WD are chemically untreated dry- and wet-densified controls. Data from [8].*

The reason is related in how the densified structure is held together. Compression brings the exposed cellulose fibril surfaces close enough for their hydroxyl groups to hydrogen-bond, and those hydrogen bonds are the only thing locking the collapsed structure in place. Water molecules are small, mobile and are themselves excellent hydrogen-bond donors and acceptors, so they compete directly for those same hydroxyl sites. Each water molecule that inserts itself into an interchain contact replaces one cellulose-cellulose bond with two cellulose-water bonds. This releases the internal stress stored during pressing without contributing anything that can transfer load across the interface, so the fibrils separate and the compression is released.

The mechanical consequence of such swelling is directly and evident. Andze and colleagues Andze and colleagues [8] found that the Young's modulus of their chemically pretreated densified specimens fell by roughly a factor of four on swelling, and their summary of dry against wet performance is given in Table 2. Their own conclusion was that densification had not produced bonds stable enough to prevent the material reverting towards its original form, and that further work on chemical bonding or impregnation would be needed. That statement is one of the direct starting point for this project.

Property	**Dry state**	**After swelling in saline**	**Cortical bone benchmark**
Bending strength	160–215 MPa (up to 2.3× untreated)	~50–60% above control, but far below dry value	~100–200 MPa
Young's modulus	6–7.2× untreated juniper	falls ~4×; K0 and K10 approach bone	~15–25 GPa
Density	up to 1300 kg m^{-3}	falls 35–45%	~1800–2000 kg m^{-3}

Table 2: *Summary of the change in mechanical performance of chemically pretreated densified juniper on passing from the dry to the swollen state, expressed relative to untreated juniper wood. Compiled from [8].*

A second barrier sits alongside the first, and it concerns what water does not do. Delignified, densified wood is mostly crystalline cellulose, and within a crystallite the β-1,4-glucan chains are packed so that the glycosidic oxygens are poorly exposed. Neutral water at body temperature hydrolyses those linkages only extremely slowly and does not break the crystal down into soluble sugars. Water therefore attacks the interfibril hydrogen bonds, which are accessible, and leaves the covalent backbone, which is not. The fibrils move apart and the strength collapses, but the cellulose itself remains in the block, still held by the hydrogen bonding of its surroundings. A soaked plate can be mechanically useless and still shed almost no measurable material.

Two implantation studies show the same behaviour in tissue. The work of Modulevsky and colleagues [14] placed plant-cellulose scaffolds in mice for eight weeks; the pieces shrank and deformed, but the authors attributed the change to collapse of empty cell-wall cavities rather than to chain scission, and concluded that the cellulose was not being degraded. In a longer study, Märtson and colleagues Märtson

and colleagues [5] left viscose cellulose sponges under rat skin for sixty weeks; the matrix cracked and the foreign-body response faded, but the polymer was still present and intact at the end.

Taken together these two barriers rule out the material in the form described. An implant is never dry. It sits in tissue at 37 °C surrounded by fluid, so the properties that determine whether it can hold a fracture are the wet-state properties, and those are the ones densified wood loses. At the same time, the material that remains after it has stopped being useful shows no sign of leaving the body, so the second operation that motivated the search for an alternative would still be required. Any useful modification therefore has to act on the junction between fibrils rather than on the cellulose itself. What is needed at that junction is a link that holds while the plate is carrying load and can be cut once it is not, which is a requirement that hydrogen bonding cannot meet and that no amount of further compression will produce.

1.4 Aim, research questions and original contribution

The aim of this project is to determine whether citric acid ester crosslinking of partially delignified, densified juniper wood can reduce swelling, preserve mechanical properties in the wet state, and introduce a degradation pathway, so as to address the barriers identified in Section 1.3 that prevent densified wood being used as a resorbable bone fixation material.

Because the investigation was carried out in two stages, it is directed by two research questions rather than one.

RQ1:

Addressed by the preliminary stage: how do the moisture state of the wood during pressing and the delignification cooking time affect the structural integrity and mechanical properties of the densified product?

RQ2:

Addressed by the main stage: how does 10 wt% citric acid crosslinking affect flexural strength and Young's modulus in the dry and swollen states, dimensional stability, chemical composition, and the rate of cellulose release into simulated body fluid?

2. Theoretical Framework and Hypothesis

2.1 Ester crosslinking and reduced water uptake

Cellulose is a linear homopolymer of β-D-glucopyranose units joined by β-1,4-glycosidic bonds. Each anhydroglucose unit carries three hydroxyl groups: two secondary alcohols at C2 and C3 on the ring, and one primary alcohol at C6 on the exocyclic –CH_2OH arm. Because oxygen is far more electronegative than either carbon or hydrogen, each of these O–H bonds is strongly polarised: the oxygen carries a substantial partial negative charge and the hydrogen a partial positive charge. Every hydroxyl is therefore simultaneously a hydrogen-bond donor, through H, and a hydrogen-bond acceptor, through the two lone pairs on its O. The glycosidic and ring oxygens add further acceptor sites. A cellulose surface is, in effect, a dense two-dimensional array of hydrogen-bonding sites, which is exactly why cellulose is hydrophilic and why wood absorbs water.

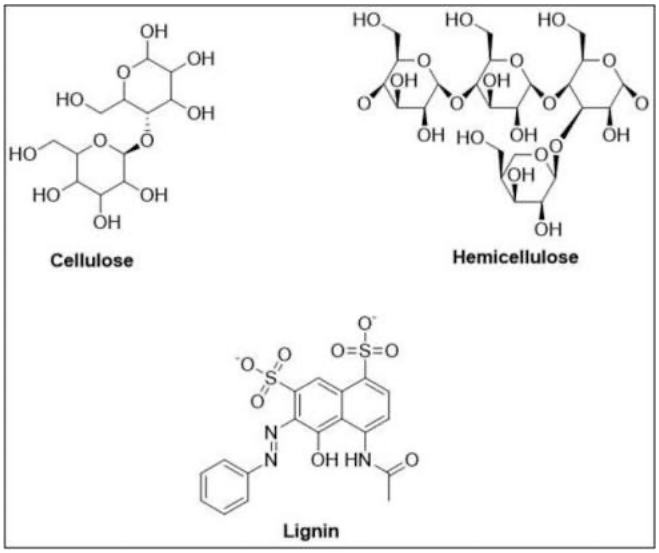


Figure 5: *Chemical structures of cellulose, hemicellulose and lignin. The regularly repeating hydroxyl groups along the cellulose chain provide both the interchain hydrogen bonding responsible for its strength and the reaction sites available for esterification [9].*

Citric acid reacts with these hydroxyls by esterification. On heating above roughly 150 °C, two adjacent carboxyl groups on the citric acid molecule undergo intramolecular dehydration to form a five-membered cyclic anhydride. This anhydride is far more electrophilic than the parent carboxylic acid and is opened by nucleophilic attack from a cellulose hydroxyl oxygen, producing an ester linkage and regenerating a free carboxyl group. That regenerated carboxyl can then dehydrate again and react with a second hydroxyl, so a single citric acid molecule can tether two or three separate chains (Figure 6). Because the reaction requires the anhydride intermediate, it will not proceed at room temperature; reported optimum curing temperatures for citric acid esterification of cellulose are

165 to 175 °C [10], which is why a high-temperature curing step is built into the method in Section 3.2.2.

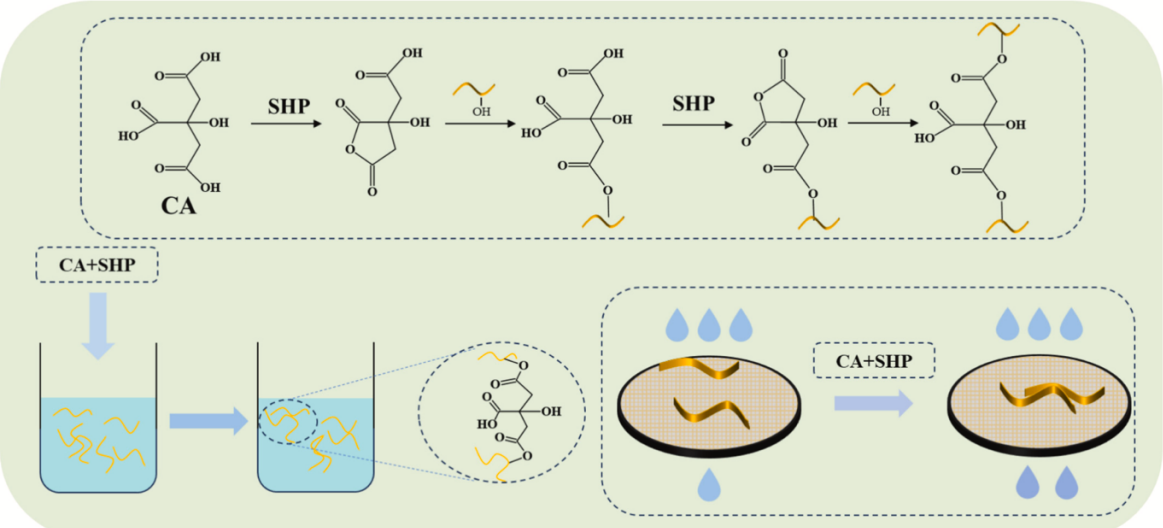


Figure 6: *Schematic of the citric acid crosslinking mechanism on cellulose fibres. Successive dehydration of adjacent carboxyl groups generates cyclic anhydride intermediates, each of which is opened by a cellulose hydroxyl to give an ester linkage [11].*

2.2 Interfacial energy analysis

The mechanical argument rests on comparing the energy of the bonds that currently carry load across a fibril interface with the energy of the bonds that crosslinking introduces. Table 3 sets out the relevant values.

Interaction	Energy (kJ mol⁻¹)	Behaviour in water at 37 °C
Interchain O–H···O hydrogen bond in cellulose I	17–30 (~20 typical)	Reversible; readily displaced by competing water molecules
C–O single bond (ester linkage)	~358	Cleaved only by hydrolysis, which is slow at neutral pH
C=O double bond (ester carbonyl)	~745	Not cleaved under physiological conditions
C–C single bond	~348	Not cleaved under physiological conditions

Table 3*: Comparison of the interactions responsible for load transfer across a cellulose–cellulose interface before and after citric acid crosslinking.*

Hydrogen bond values from [13]; bond enthalpies are standard tabulated averages.

A single ester C–O linkage is therefore worth roughly eighteen interchain hydrogen bonds on an energy basis. That ratio alone is not the whole story, because the hydrogen bonds are far more numerous, so the comparison has to be made per unit of interfacial area rather than per bond. [13] gives the areal number density of hydrogen bonds on the (1–1 0) crystallographic plane of cellulose I as approximately 3.7×10^{18} m^{-2}. The work required to separate two such surfaces against the hydrogen-bond network is then

$$G_h = (20 \times 10^3 \text{ J mol}^{-1} \times 3.7 \times 10^{18} \text{ m}^{-2}) / (6.022 \times 10^{23} \text{ mol}^{-1}) \approx 0.12 \text{ J m}^{-2}$$

Now apply the degree of esterification represented in the model of Section 2.1. That model contains twelve citrate bridges forming twenty-four ester linkages across three chains of eight anhydroglucose units, which carry seventy-two hydroxyl sites in total, so one third of the available sites are converted. Taking the site density as unchanged, the areal density of covalent junctions is $0.33 \times 3.7 \times 10^{18} \approx 1.2 \times 10^{18}$ m^{-2}. The corresponding contribution to the work of separation, taking 358 kJ mol^{-1} for the C–O bond, is

$$G_e = (358 \times 10^3 \text{ J mol}^{-1} \times 1.2 \times 10^{18} \text{ m}^{-2}) / (6.022 \times 10^{23} \text{ mol}^{-1}) \approx 0.73 \text{ J m}^{-2}$$

The remaining two thirds of the hydrogen bonds still contribute $0.67 \times 0.12 \approx 0.08$ J m^{-2}, so the total interfacial work in the dry state comes to roughly 0.81 J m^{-2} against 0.12 J m^{-2} for the untreated interface. Two qualifications are needed. The one-third figure is the degree of substitution drawn in the model, not a measured quantity; the true degree of esterification in a pressed specimen is unknown, and the ester-to-cellulose peak-area ratios reported in Section 4.1 are spectroscopic ratios rather than a degree of substitution. More importantly, interfacial work and strength are not the same quantity. Strength also depends on the flaw population, on fibril alignment and on how far the material can be compacted, none of which this calculation captures and all of which crosslinking is expected to alter. The figures above should therefore be read as an order-of-magnitude comparison between two kinds of interface, not as a prediction of how strong the material will be.

It should be said at the outset that this treatment assumes every modelled crosslink actually forms and that each contributes its full bond energy to the interface. Both assumptions are generous and is purely theoretical. The calculation therefore sets an upper bound on what esterification could deliver, and the comparison between that bound.

The far more important prediction concerns the wet state. Water attacks the hydrogen-bonded term and leaves the covalent term untouched. In the limit where water has displaced essentially all of the interchain hydrogen bonds, the untreated material retains almost nothing of G_h, whereas the crosslinked material retains the full 0.73 J m^{-2} of G_e. The expected outcome is therefore not a uniform improvement but a change in the shape of the dry-to-wet transition: a modest gain, or possibly even a loss, in absolute dry strength, combined with a much larger proportional gain in the fraction of that strength retained

after swelling. This is the specific, falsifiable prediction that the mechanical testing programme is designed to test.

The possibility of a dry-state loss deserves explanation, because it follows from the chemistry rather than being an experimental accident. Citric acid is an acid, and the curing step holds the specimen at 160 to 165 °C in an acidic environment. Under those conditions the β-1,4-glycosidic bonds of cellulose and hemicellulose are themselves susceptible to acid-catalysed hydrolysis. Chain scission lowers the degree of polymerisation, which reduces the length over which load can be transferred along a chain and therefore reduces strength. Tao and Nonaka (2021) note that citric acid concentration and curing conditions both have to be controlled for this reason, and Huang et al. (2024) observed that excessive citric acid reduced pulp performance and increased fine content precisely through acid hydrolysis of cellulose. There are thus two competing effects operating on the same variable: increasing citric acid concentration adds crosslinks, which strengthen the interface, and simultaneously promotes chain scission, which weakens the chains. A concentration of 10 wt% was selected as a starting point within the range commonly reported to give effective crosslinking without severe hydrolysis [12].

2.3 Ester links as a path for degradation

The third argument is that the same chemical change that stabilises the material against water also gives it a way to disappear. To see why, it is worth restating exactly what is wrong with the untreated material, because the problem is not that water cannot get in.

In densified, delignified wood the fibrils are held together by a dense, ordered network of hydrogen bonds between hydroxyl groups. Water penetrates that network easily, because the interface is highly polar, and inserts itself between the chains. But having got in, it has nothing to attack. The covalent backbone of cellulose is a chain of β-1,4-glycosidic acetal linkages, and acetals are hydrolysed only under acid catalysis or by an enzyme; at pH 7.4 and 37 °C the uncatalysed rate is negligible on any clinically relevant timescale, and mammals do not produce cellulase [14]. The adsorbed water therefore simply forms hydrogen bonds with the cellulose and remains where it is. It is strongly enough bound to prise the fibrils apart, which is what produces the swelling and the loss of strength, but it cannot separate them, because the fibrils remain long, crystalline and mutually hydrogen-bonded over their whole length. In effect, water gets all of the destructive consequences and none of the useful ones.

Crosslinking changes the identity of the link that has to be broken. After esterification, a substantial share of the load-bearing junctions between chains is no longer a hydrogen bond but an ester. Esters are hydrolysable: attack of water at the carbonyl carbon regenerates a carboxylic acid and an alcohol. Under physiological conditions this reaction is slow, which is exactly what is required, because the implant has to remain intact for the six to eight months of bone healing rather than dissolving in the first weeks. But it is not negligible, and unlike acetal hydrolysis it does not require an enzyme the body does not

possess. Ester hydrolysis is the same mechanism that governs the resorption of established degradable orthopaedic polymers such as poly(lactic acid), which is why those materials resorb over months while cellulose does not [15].

Figure 7 sets the two routes side by side. In the untreated material (route A) water enters, hydrogen-bonds, swells the structure and stops. In the crosslinked material (route B) water enters and cuts tethers. Each ester that hydrolyses regenerates one free carboxyl on the citric acid residue and one free hydroxyl on the cellulose. Those newly liberated hydroxyls are immediately solvated by the surrounding water rather than re-forming a dry contact with the neighbouring fibril, so the junction does not simply reseal. As tethers are progressively cut, individual fibrils are released from the compacted mass, the accessible surface area rises sharply, and the fragments become small enough to be taken up by macrophages and cleared, which is the route by which cellulose-based implants are known to be removed in vivo in the absence of cellulase.

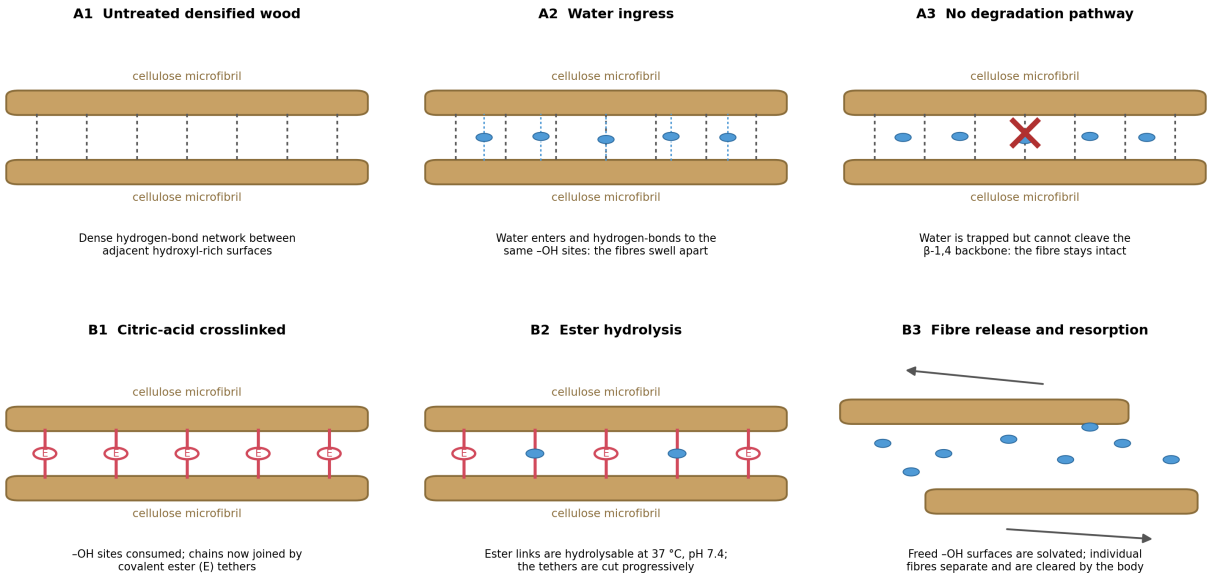


Figure 7: *Proposed contrast between the two degradation routes. Route A (top): in uncrosslinked densified wood, water penetrates the hydrogen-bonded interface and swells the structure, but has no covalent linkage available to cleave, so the fibril network stays intact. Route B (bottom): after citric acid crosslinking the interfibrillar junctions are hydrolysable esters, which are cut progressively at 37 °C and pH 7.4, releasing individual fibrils for solvation and clearance.*

Three further points support this route. First, the products are benign, hydrolysis returns citric acid, an intermediate of the citric acid cycle present in every human cell, and cellulose fragments that are ultimately reduced to glucose units. Second, the reaction is mildly self-accelerating, because each cleaved ester leaves behind a carboxylic acid that lowers the local pH and can catalyse further hydrolysis, a behaviour also seen in polyester implants. Third, and most usefully for design purposes, the rate is tunable. Because the number of hydrolysable links is set by the degree of esterification, and the degree of esterification is set by citric acid concentration and curing conditions, the same processing variable

that controls wet-state strength also controls degradation rate. The material is not simply being made degradable; it is being made degradable in a way that can be adjusted.

Taken together, Sections 2.1 to 2.3 can provide a hypothesis which states that replacing part of a reversible, hydroxyl-mediated interface with covalent but hydrolysable ester linkages should reduce swelling, improve the retention of mechanical properties in the wet state, and introduce a degradation pathway where none previously existed, through acid-catalysed chain scission during the treatment.

3. Methodology

The fabrication route has three stages: mechanical preparation of the raw wood, chemical treatment consisting of partial delignification followed by citric acid crosslinking, and hot pressing. The route was assembled from the delignification and densification conditions of Song et al. (2018) and [8] and the citric acid curing conditions reported for cellulosic materials, and was then adapted to the equipment and safety constraints of the laboratory available.

3.1 Preparation

3.1.1 Juniper wood

Common juniper (Juniperus communis) was selected as the raw material. The choice was made on biological reasons.

A central obstacle to use natural wood in the body is the immune response. The body recognizes an implanted material through the proteins that adsorb onto its surface, and the chemically varied surface of natural wood, rich in lignin and assorted extractives, tends to provoke a strong reaction in which immune cells attach to the rough, porous surface and can drive chronic inflammation. For most species, reducing this response would require additional chemical extraction to remove the reactive components.

In this study, Juniper (*Juniperus communis*) was selected because Gross and Ezerietis (2003) reported have demonstrated that it possesses an unusually favourable combination of mechanical properties and biological compatibility [17]. In one of the earliest investigations of wood as an implant material, Gross and Ezerietis (2003) reported that juniper contains naturally occurring essential oils with antiseptic and antibacterial properties. Their study found that implanting untreated Juniper wood into rabbits demonstrated good biological acceptance for periods of up to three years, with evidence of bone apposition, tissue attachment and bone growth into the porous structure of the wood. These findings suggested that unlike other wood, juniper could function as an implant material without provoking significant adverse biological reactions.

Timber certification for the material used is shown in Figure 8. Blocks were supplied pre-cut at approximately 81 × 16 × 16 mm and were visually inspected on arrival; any piece containing a major crack or knot was discarded, since such defects act as stress concentrators and would make bending results meaningless.

木材质量保证书

参数类别	具体参数	详情
产品基础参数	材质种类	杜松
	91mm*16mm*16mm	
	等级	按行业标准
	生产批次/编号	2026/4/3-/GFMY0156
物理性能参数	含水率	30%以下
	密度/气干密度	0.40~0.50
	顺纹抗压强度、抗弯强度	46.7MPa/81.1MPa
质量缺陷控制参数	外观缺陷	不允许腐朽、虫蛀、死节
	加工质量	精品质量
合规性参数	执行标准	产品符合的国家/行业标准编号GB/T 4817-2015《实木锯材》
	环保指标	室外符合行业标准
检测相关参数	检测依据	出厂自检
	检测日期	2026/4/3
出货单位	太仓古方木业有限公司	

Figure 8: *Timber Information & Quality Certification for the Juniper Wood Used in This Project*

3.1.2 Sanding

Every block was sanded on all six faces to bring it to a final dimension of 80.0 ± 0.1 mm (length) × 14.2 ± 0.1 mm (width) × 15.0 ± 0.1 mm (height). Sanding proceeded sequentially through 120-, 240- and 400-grit papers, with dust removed by brush or compressed air after each stage, and the finished dimensions of every specimen were measured with a digital calliper and recorded before the specimen was labelled.

3.1.3 Mould design

Producing consistent densified wood requires each specimen to be compressed under a controlled and repeatable pressure, and this cannot be achieved by pressing between flat platens alone. In one of Nile Red's Youtube video, a block compressed without lateral constraint expands sideways as it is squeezed, as shown in Figure 9A and 9B. That lateral flow has three consequences. First, the specimen never reaches the intended degree of through-thickness compression. Second, the applied load is dissipated in deformation rather than densification. Third, the finished specimens have irregular and inconsistent dimensions, which makes any subsequent comparison between treatment conditions impractical. A closed compression mould was therefore designed and machined to constrain the

specimen on all four sides, so that the applied load produces through-thickness densification only (Figure 9C and 9D).

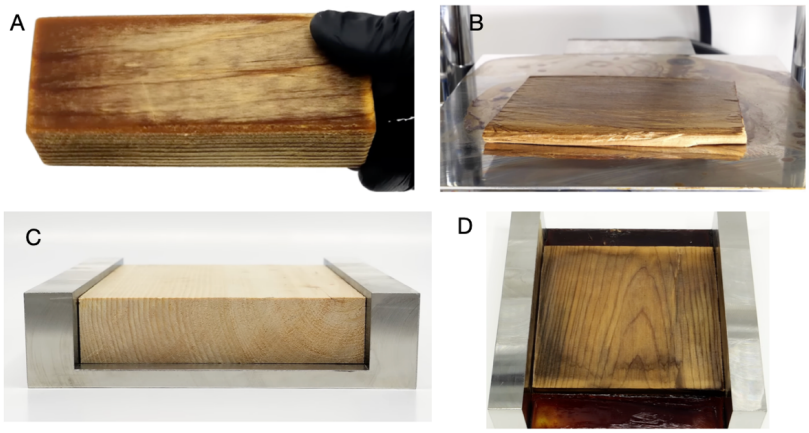


Figure 9: *Comparison of wood compressed without and with a closed mould. (A) Original block before pressing without a mould. (B) The same block after pressing, showing lateral expansion and irregular edges. (C) A block placed inside a closed mould before pressing. (D) The same block after pressing, showing constrained lateral dimensions and uniform through-thickness densification [7].*

The mould was machined from stainless steel for its strength, dimensional stability and resistance to the temperature and moisture of the hot-pressing cycle, and was designed with three parallel channels so that three trials of each condition can be densified in a single cycle (Figure 10).

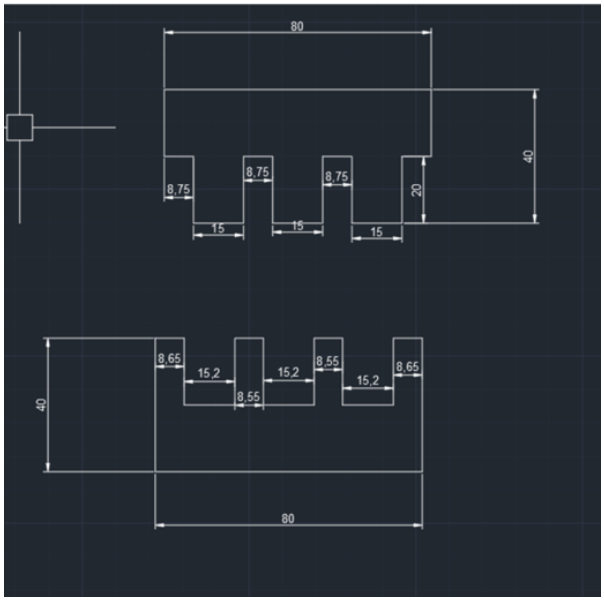


Figure 10: *Three-cavity stainless steel compression mould designed for this project.*

Because a hydraulic press is set by total force, the required press load had to be calculated for the geometry of the three-cavity mould. Therefore, careful calculation for letting each piece pressed with 5 Mpa is calculated. Taking the loaded face of a single specimen as 80.0 mm × 14.2 mm:

$$A_1 = L \times W = 0.080\ \text{m} \times 0.0142\ \text{m} = 1.136 \times 10^{-3}\ \text{m}^2$$

$$A = 3A_1 = 3.408 \times 10^{-3}\ \text{m}^2$$

$$F = PA = (5 \times 10^6\ \text{Pa})(3.408 \times 10^{-3}\ \text{m}^2) = 1.704 \times 10^4\ \text{N}$$

$$F = (1.704 \times 10^4) \div (9.80665 \times 10^3) \approx \mathbf{1.74\ tonne\text{-}force}$$

The press was therefore set to approximately 1.74 tonne-force for every three-specimen cycle, so that each specimen experiences the intended 5 MPa regardless of the total force shown on the gauge.

3.2 Chemical treatment

3.2.1 Delignification

Delignification selectively removes much of the lignin and hemicellulose while preserving the cellulose framework, and it is what makes densification possible at all. Lignin is a rigid, crosslinked three-dimensional aromatic polymer that fills the space between the cellulose microfibrils and acts as the glue holding the cell wall rigid; while it is intact the cell walls resist collapse and the wood cannot be compressed. Hemicellulose is a branched, amorphous polysaccharide that forms the matrix around the microfibrils and is chemically the least stable of the three components, so it is removed most readily.

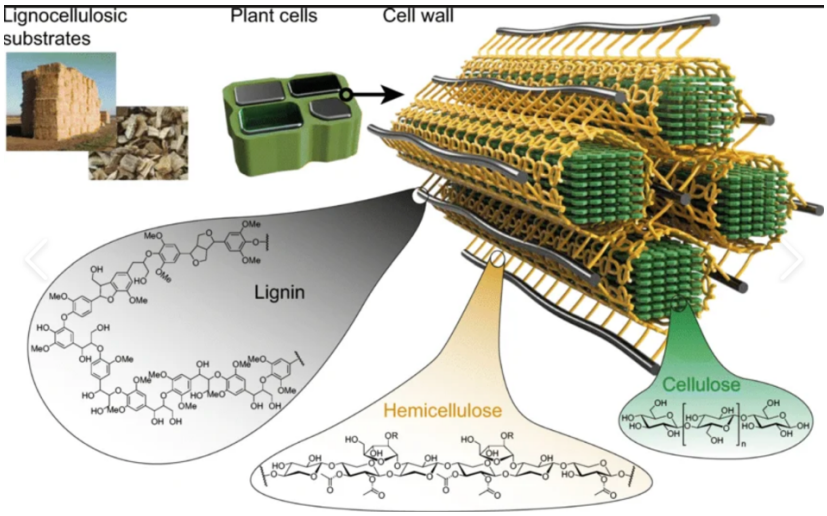


Figure 11: *Architecture of the lignocellulosic cell wall, showing crystalline cellulose microfibrils embedded in a hemicellulose matrix and encased in lignin. Delignification removes the lignin and much of the hemicellulose, opening the wall and exposing the cellulose hydroxyl groups.*

The cooking liquor used here was aqueous 2.5 M sodium hydroxide with 0.4 M sodium sulfite, following Song et al. (2018). Prepared in 1.0 L batches, this requires 100.00 g of NaOH pellets and 50.41 g of anhydrous Na_2SO_3. The NaOH is added slowly to approximately 800 mL of stirred deionised water, which is strongly exothermic, and the solution is allowed to cool before the Na_2SO_3 is added and dissolved; the mixture is then made up to 1.0 L in a volumetric flask. The two reagents act by different mechanisms. Sodium hydroxide swells the cell wall and opens up the structure, and it also saponifies

the acetyl side groups on hemicellulose; those acetyl groups are hydrophobic and are what keeps hemicellulose from dissolving, so their removal leaves hydroxyl groups in their place, which are then deprotonated in the alkaline medium. The resulting negatively charged hemicellulose fragments repel one another electrostatically and hydrate preferentially, in this way, they dissolve. Sodium sulfite dissociates in water to give sulfite ions, which act as nucleophiles and cleave the β-O-4 ether linkages of lignin by sulfonation, converting it into soluble lignosulfonate fragments that can be washed out.

Cellulose is largely untouched by both processes. Its glycosidic C–O–C linkages are acetal-like and comparatively unreactive towards hydroxide and sulfite, and its highly ordered crystalline packing makes it difficult for the alkaline solution to penetrate in the first place. It is also shown by Song et al. (2018) that in basswood, chemical treatment reduced lignin from 20.8% to 11.3% and hemicellulose from 19.5% to 5.2% while cellulose fell only from 44.0% to 38.7% [6].

In practice, sanded specimens are placed inside a enclosed glass bottle and fully submerged in the delignification solution, then left to impregnate at room temperature for 12 hours so that the solution reaches the interior of the block before any reaction is driven thermally. The glass bottle is then opened (so that no pressure can accumulate) and transferred to a water bath heated up to 100 degrees Celsius, and cooked for the required duration. A thermometer is place inside the glass bottle which contains the sample and cooking time initiates as soon as the solution reaches 100 degrees Celsius. Cooking times of one to five hours define conditions K1 to K5.

Delignification is intentionally only partial, and the choice of cooking time range was made experimentally. Too little removal leaves the cell walls too rigid to densify; too much destroys the structural integrity of the wall and weakens the densified product. Song et al. (2018) found the highest strength at an intermediate degree of delignification (K3-K4). A preliminary test across six cooking times, K1 to K6, was therefore carried out for juniper. Flexural strength rose from 88.9 MPa for undelignified control wood to a maximum of 354.7 MPa at K5 and then fell at K6 (Figure 12), so K6 was excluded and the main investigation was restricted to K1 to K5. This choice is further discussed in the acknowledgement.

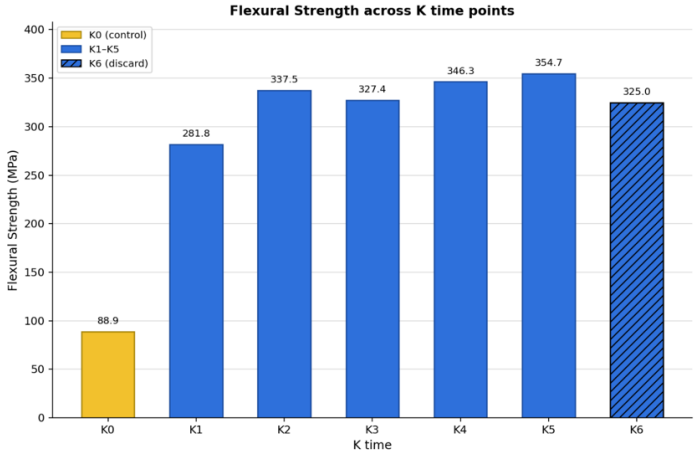


Figure 12: *Flexural strength of densified juniper across the preliminary screen of delignification cooking times. K0 is the undelignified control; K6 was discarded because strength had begun to decline.*

Washing and neutralisation follow, and they are more demanding than they appear because any residual alkali left in the specimen will interfere with the acid-catalysed esterification in the next stage and would be unacceptable in a material intended for implantation. Specimens are transferred to a large beaker and washed repeatedly with warm deionised water at approximately 80 °C until the wash water reads pH 7-8. Finally the washes are switched to room-temperature deionised water and repeated until two consecutive washes in two days read pH 7.00 ± 0.10 on a calibrated meter. Washed specimens are stored submerged in fresh deionised water.

3.2.2 Citric acid crosslinkage

Crosslinking is carried out after delignification and before pressing, which is chosen specifically. Delignified wood has open pores of roughly 10 to 50 μm and freshly exposed hydroxyl groups, so citric acid solution can penetrate throughout the block; once the material has been densified those pores are gone, any subsequent treatment would only modify the surface. Crosslinking before compression also means the network is chemically locked as it is compressed, which should reduce spring-back effect.

A 10 wt% citric acid solution is prepared in deionised water, warming gently until clear, and the washed delignified specimens are fully submerged in it for 24 hours. Curing is carried out by placing the specimens on non-stick trays in a drying oven at 170 °C for 90 minutes. After curing the oven is switched off and the specimens are allowed to cool inside with the door open, which avoids thermal shock and condensation. They are then rinsed with deionised water at approximately 25 °C to remove unreacted citric acid on the surface, and dried to constant mass at 60 °C inside a oven (do not contact with water for too long or use heated water, since it might cause degradation of the ester bonds).

The temperature window is also selected with scientific context. As set out in Section 2.1, esterification proceeds through a cyclic anhydride intermediate that only forms once citric acid dehydrates, and reported optimal temperature for citric acid esterification of cellulose lie at 170 °C [10]. Curing below roughly 150 °C would leave the citric acid largely unreacted, so that it acts as a soluble additive rather than a crosslinker and simply washes out; curing much higher risks charring and accelerates acid-catalysed hydrolysis of the polysaccharide chains.

The concentration of 10 wt% was selected as the single crosslinking condition for the main investigation, for the reasons given in Section 2.2: concentrations in this range are commonly reported to give effective crosslinking and improved water resistance [12], while higher concentrations increase the risk that acid-catalysed chain scission during curing damages the structure and strenght of pieces.

3.3 Hot pressing

Densification is carried out at 100 °C under 5 MPa for approximately 24 hours, following Song et al. (2018) and [8], with the specimens loaded into the three-cavity stainless steel mould described in Section 3.1.3 and the press set to the 1.74 tonne-force as calculated. After the hold period the assembly is cooled while still under full pressure and the load is then released slowly; releasing pressure while the specimen is still hot allows elastic recovery before the structure has set. Final dimensions and mass are recorded immediately so that the densified density can be calculated.



Figure 13: *Specimens loaded into the three-cavity mould before hot pressing.*

3.4 Experimental design and specimen groups

Three materials are compared in this report, and the naming used here is carried through the Results and Discussion. Untreated juniper is the raw feedstock, taken through no chemical or mechanical treatment. DW denotes densified wood: juniper partially delignified and hot pressed, with no citric acid step. CA-DW denotes citric acid crosslinked densified wood: the same material with the 10 wt% citric acid impregnation and 170 °C cure of Section 3.2.2 inserted between washing and pressing. DW is the control against which CA-DW is judged.

Within each treated group, K1 to K5 denote delignification cooking times of one, two, three, four and five hours. Both groups were prepared from the same stock of juniper, delignified for the same five times, washed to the same endpoint and pressed under identical conditions, so that the only variable distinguishing DW from CA-DW is the crosslinking step itself. Three replicate specimens were prepared for each combination of group and delignification time, and every reported value is the mean of those replicates.

Group	Delignification	Citric acid step	Hot pressing	Purpose
Untreated juniper	None	None	None	Raw-material baseline
DW	2.5 M NaOH / 0.4 M Na_2SO_3, 1–5 h	None	100 °C, 5 MPa, 24 h	Control

CA-DW	2.5 M NaOH / 0.4 M Na_2SO_3, 1–5 h	10 wt%, 24 h soak, cured 165–170 °C for 2 h	100 °C, 5 MPa, 24 h	Experimental group

Table 4: *Specimen groups and the treatment each received. DW and CA-DW differ only in the citric acid step.*

3.5 Characterisation

Characterisation was divided between tests that could be carried out reliably in the laboratory established for this project and tests requiring instrumentation that was not available. Infrared spectroscopy, three-point bending and scanning electron microscopy were performed by the Shaanxi Coal Chemical Industry Technology Research Institute on specimens prepared and supplied by the authors; the swelling and degradation measurements were carried out by the authors. Because several of the mechanical tests are destructive, the order of testing was planned so that flexural strength, the single most relevant property for a fixation plate, was measured first, with the remaining measurements taken on the resulting fragments.

3.5.1 Infrared spectroscopy

Dried specimens were ground to a fine powder before analysis, one specimen per delignification group in each batch. Spectra were recorded by the external institute. Peak areas were integrated for the lignin aromatic band, the ester carbonyl band at 1715–1745 cm^{-1} and the cellulose C–O band at 1000–1100 cm^{-1}, the last of which is unaffected by either treatment and was therefore used as an internal standard so that absolute peak area would not depend on the quantity of powder analysed. Composition is reported as the ratio of the lignin or ester band to the cellulose band.

3.5.2 Mechanical testing

Flexural strength, maximum load and Young's modulus were measured in three-point bending by the external institute, in both the dry state and after swelling to equilibrium. Specimens for wet-state testing were kept sealed in saline until the moment of testing so that they would not dry out in transit or handling.

3.5.3 Swelling

Specimens were first oven dried to constant mass, then immersed in 0.9% saline held at 37 °C, a solution chosen because its osmolarity approximates that of body fluid. Each specimen was removed, surface blotted and weighed at two-hour intervals until the change in mass between successive weighings fell below 0.05 g, which was taken as the point of equilibrium swelling. Dimensions were measured with digital callipers before immersion and at equilibrium, and volume was calculated from those dimensions; mass uptake and volume increase are reported as percentages of the dry values. Three replicates were run for each condition.

3.5.4 Degradation assay

Degradation was quantified as the mass of cellulose released from a specimen into simulated body fluid, for the reasons set out in Section 2.3. Each specimen was placed in a 50 mL container, simulated body fluid was added until the specimen was fully submerged to a total contents volume of approximately 60 mL, leaving roughly 55 mL of free liquid once the volume displaced by the specimen is allowed for, and the sealed container was held at 37 °C for ten days.

Cellulose released into the medium consists largely of long chains with few free reducing ends and gives little colour with 3,5-dinitrosalicylic acid, so it was first hydrolysed enzymatically. A 10.0 mL aliquot of the immersion liquid was taken, 80 mg of cellulase powder (2000 U g^{-1}) was added and dispersed, and the mixture was incubated at 50 °C for approximately 24 hours, this being the working temperature of the enzyme. The cellulase acts here purely as an analytical reagent and is not intended to simulate any process occurring in the body. The hydrolysate was then centrifuged and filtered to remove residual enzyme powder and particulates.

For colour development, 10.0 mL of the clarified hydrolysate was mixed with 15.0 mL of DNS reagent, a sample-to-reagent ratio of 2:3, and heated at 100 °C for 20 minutes in a boiling water bath. Under alkaline conditions at high temperature the aldehyde group of each reducing sugar is oxidised to a carboxylic acid while 3,5-dinitrosalicylic acid is reduced to 3-amino-5-nitrosalicylic acid, giving an orange-red product whose intensity is proportional to the quantity of reducing sugar present. Tubes were cooled and left overnight for the colour to develop fully, then filtered before measurement.

Absorbance was read at 540 nm, the absorption maximum of the coloured product, with each sample measured three times. A calibration curve was constructed from glucose standards at 0.1, 0.2, 0.3, 0.4 and 0.5 mg mL^{-1}, each carried through the identical colour reaction in triplicate, the range being chosen to span the absorbances expected from the samples so that all sample concentrations could be obtained by interpolation rather than extrapolation. Glucose concentrations were converted back to the mass of cellulose from which they derived by multiplying by the ratio of the anhydroglucose repeat unit to glucose, 162.14/180.16 = 0.900, which accounts for the water added at each glycosidic bond cleaved. Untreated juniper was carried through the entire procedure as a reference.

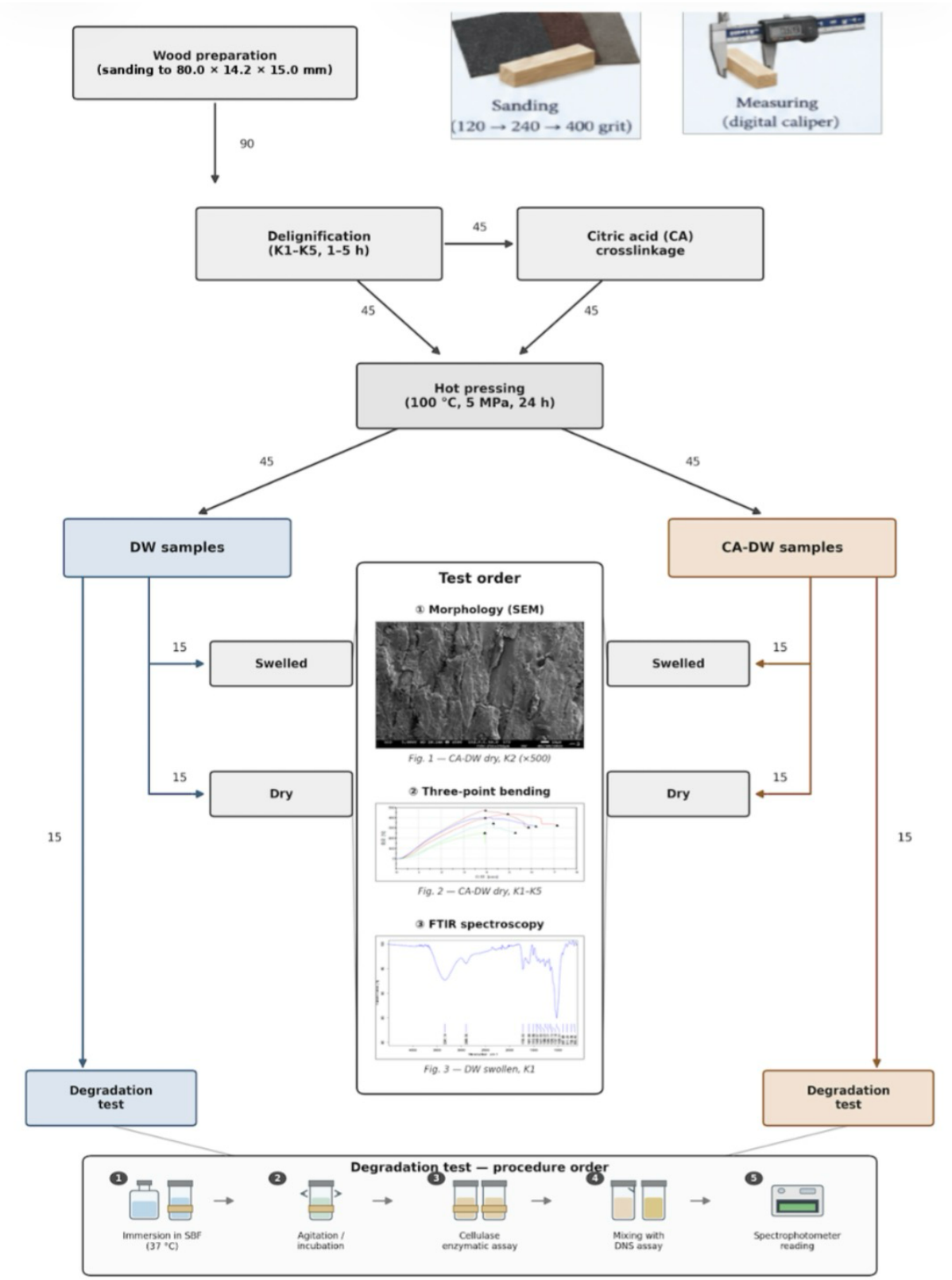


Figure 14: *A visual overview of the entire procedure of the investigation.*

4. Results

Three materials are compared throughout. Control is untreated juniper wood. DW is densified wood, partially delignified in 2.5 M NaOH / 0.4 M Na_2SO_3 and hot-pressed at 100 °C and 5 MPa. CA-DW is the same material as DW but with a 10% citric acid impregnation and a 165 °C thermal cure inserted between delignification and pressing. Within each treated group, K1 to K5 refers to delignification times of one to five hours. DW and CA-DW were prepared from the same wood, delignified for the same times and pressed under identical conditions, so they differ only in the crosslinking step and every difference between them is attributable to that step alone.

4.1 Evidence of ester formation

Infrared spectroscopy establishes that the intended reaction took place. CA-DW shows an absorption at 1715–1745 cm^{-1} that is entirely absent from DW (Figure 15a). This is the ester carbonyl stretch, and it is the direct signature of a covalent bond between a carboxyl group of citric acid and a hydroxyl group of the wood. The assignment is clear here because the only other component of wood that absorbs in this region, the acetylated hemicellulose carbonyl near 1730 cm^{-1}, has already been removed during delignification; its disappearance is itself visible in both spectra and confirms that the alkaline sulfite treatment worked as intended.

Further more, several more observation further proved the formantion of crosslinkage and reduced polarity of the mateiral. Firstly, the OH peak is significantly reduced on CA-DW compared to DW. This directly proves that OH sites on cellulose or other wood composition are consumed to be used for C=O bond instead. Secondly, reduced C-O and C-O-C peak on CA-DW also proves that C_6 – OH is now an ester, so that C–O oscillator changed.

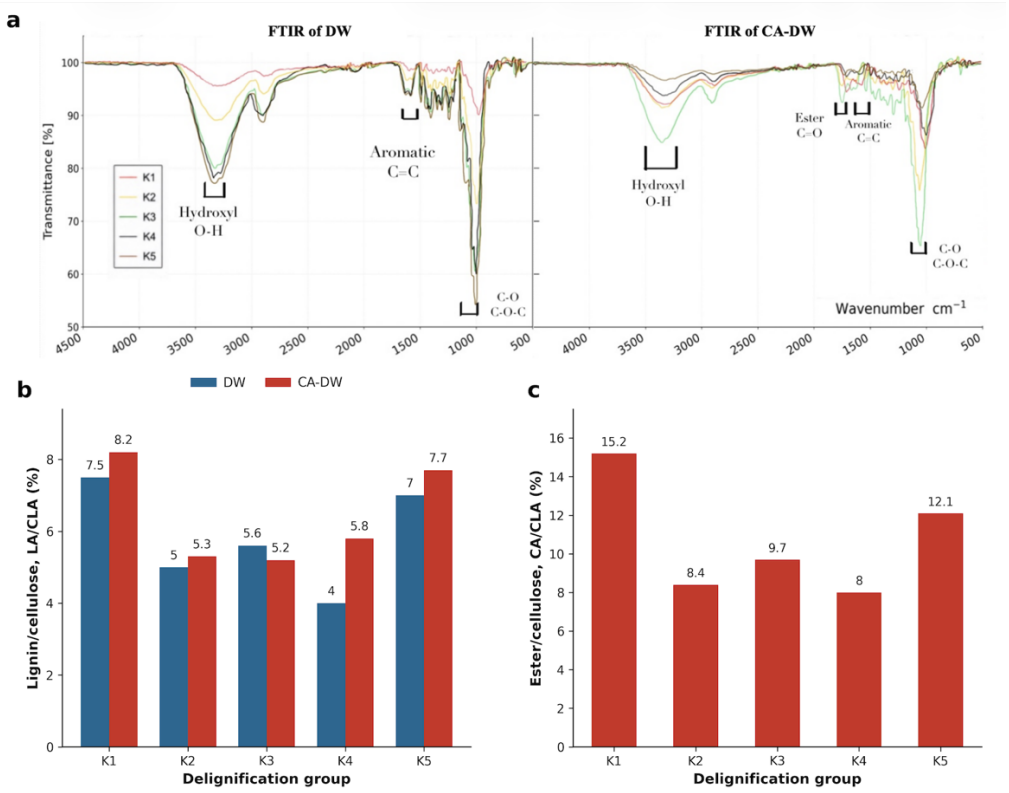


Figure 15: *Chemical evidence of ester crosslinking. (a) FTIR spectra of DW (left) and CA-DW (right) across K1–K5. (b) Lignin-to-cellulose ratio, showing equivalent delignification in both groups. (c) Ester-to-cellulose ratio, absent in DW.*

For quantitative comparison, peak areas were normalised against the cellulose C–O band at 1000–1100 cm^{-1}. Cellulose is largely preserved by both treatments, so this band serves as an internal standard and removes the dependence of absolute peak area on the quantity of powder analysed. Two ratios follow. The lignin-to-cellulose ratio (LA/CLA) converges on 4–8% in both groups and follows the same trend with cooking time (Figure 15b). This is an essential control rather than an incidental observation: it demonstrates that the two groups were delignified to a comparable extent, and therefore excludes unequal lignin removal as an explanation for any later difference between them. The ester-to-cellulose ratio (CA/CLA) is measurable at every delignification level, ranging from 8.0% to 15.2% (Figure 15c), showing that crosslinking proceeded under all conditions tested and was not confined to lightly or heavily delignified specimens. (OH bonds peak difference)

LA/CLA does not fall in a clean straight line with cooking time, and that is expected for this design. This is due to two material facts. First, K1–K5 were not five slices from one homogeneous block. Juniper lignin content varies with where it is; some parts of wood might contain higher lignin than other eventhough it is from same individual. The cooking time is not linear to lignin content becasuse the starting lignin are not fixed. Second, LA/CLA is lignin relative to the cellulose reference band. If two pieces have the same residual lignin but different cellulose packing after pressing, CLA changes and

the ratio moves. A cellulose-rich, well-densified strip can look “low lignin” even when some lignin is still there; a poorly packed strip can look high lignin content with the same cook.

Hence lignin-specific trends were plotted against LA/CLA, not against cooking time. LA/CLA is a spectroscopic estimate of leftover lignin relative to the cellulose reference band. Cooking time is only a process setting; it is not a lignin concentration.

Cooking time was still used when the question was overall mechanical behaviour. The cook does more than strip lignin. It also removes hemicellulose, opens the cell wall, and holds the tissue in hot alkali for a longer period, so packing, fibril mobility and the later press response all change. A mechanical point plotted against K-time therefore reflects that whole history, not a lignin-only effect.

Moreover, it is found that CA/CLA and LA/CLA ratios are highly related according to Figure 15b. This is because citric acid does not esterify only cellulose C6–OH. Lignin has aliphatic and phenolic OH. A piece that still has more lignin after the cook has more of those extra OH sites, so the 1730 cm^{-1} ester band can rise with LA/CLA even if cellulose accessibility is not better.

4.2 Densification change

Scanning electron microscopy shows the structural transformation on which the whole process depends. Untreated juniper presents open, hollow tracheid lumina arranged in the regular honeycomb characteristic of a softwood (Figure 16a). After delignification and pressing these lumina are entirely collapsed, both DW (Figure 16b) and CA-DW (Figure 16c) show densely packed, intertwined cell-wall material with no residual porosity.

The quantitative measurements showed the pression more directly. Pressing reduced the original 17.04 cm^3 specimen to a mean of 6.02 cm^3 for DW and 8.17 cm^3 for CA-DW, factors of 2.8 and 2.1 (Figure 16d). Dry density rose from 0.432 g cm^{-3} for untreated juniper to 1.132 g cm^{-3} for DW and 0.972 g cm^{-3} for CA-DW (Figure 16e), and volume reduction averaged 64.7% against 52.1% (Figure 16f). Across every one of the five densification levels, DW compacted further than CA-DW.

The mechanism underlying this effect involves ester bridges formed before pressing occurs. These ester bridges crosslink adjacent cell-wall polymers and increase cell wall stiffness, such that less deformation occurs under a given applied pressure.

Although this specific sequence of crosslinking before pressing gives rise to the observed reduction in compressive deformation, this processing order is deliberately chosen. Impregnating an already densified specimen cannot modify its interior structure; once the lumina have closed, reagent access is limited to the surface, resulting in a surface coating rather than the bulk cross-linkage that we are looking for.

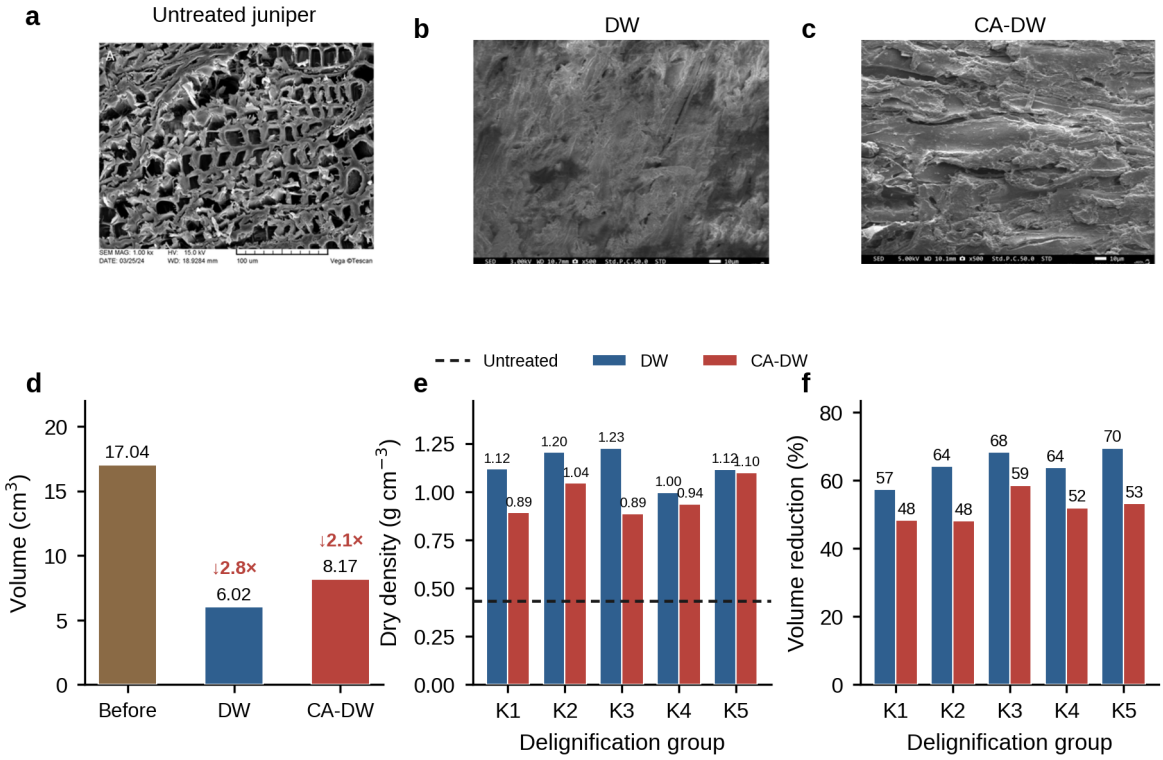


Figure 16: *Microstructure and densification. (a) SEM at ×1000 of untreated juniper. (Andze et al., 2024) (b-c) SEM of DW and CA-DW at ×500, both K5, dry. (d) Mean volume before and after pressing. (e) Dry density, untreated juniper dashed. (f) Volume reduction on pressing.*

4.3 Swelling and dimensional change

Specimens were immersed in 0.9% saline at 37 °C, chosen to approximate the osmolarity and temperature of body fluid, and weighed at two-hour intervals until successive measurements differed by less than 0.1 g. DW swelled by 101.9% in volume and absorbed water equal to 130.4% of its dry mass, meaning that it more than doubled in size and took up more water than the specimen itself weighed. Crosslinking reduced these to 73.2% and 92.0%, decreases of 28.2% and 29.4% respectively (Figure 17a, b).

These findings provide the most direct evidence that crosslinking alters the material's interaction with water, and the underlying mechanism aligns with the background rationale. Esterification consumes hydroxyl groups, which serve both as water-binding sites and as the structural basis of the hydrogen-bond network disrupted by water uptake. Depletion of these groups reduces the driving force for water absorption, while the covalent bridges that take their place constrain the dimensional swelling that would otherwise result from water uptake.

This reduction was observed across four out of the five delignification levels. The only exception was the K1 condition, where mass uptake values for the two groups fell within 3% of one another.

4.4 Mechanical properties and swelling retention

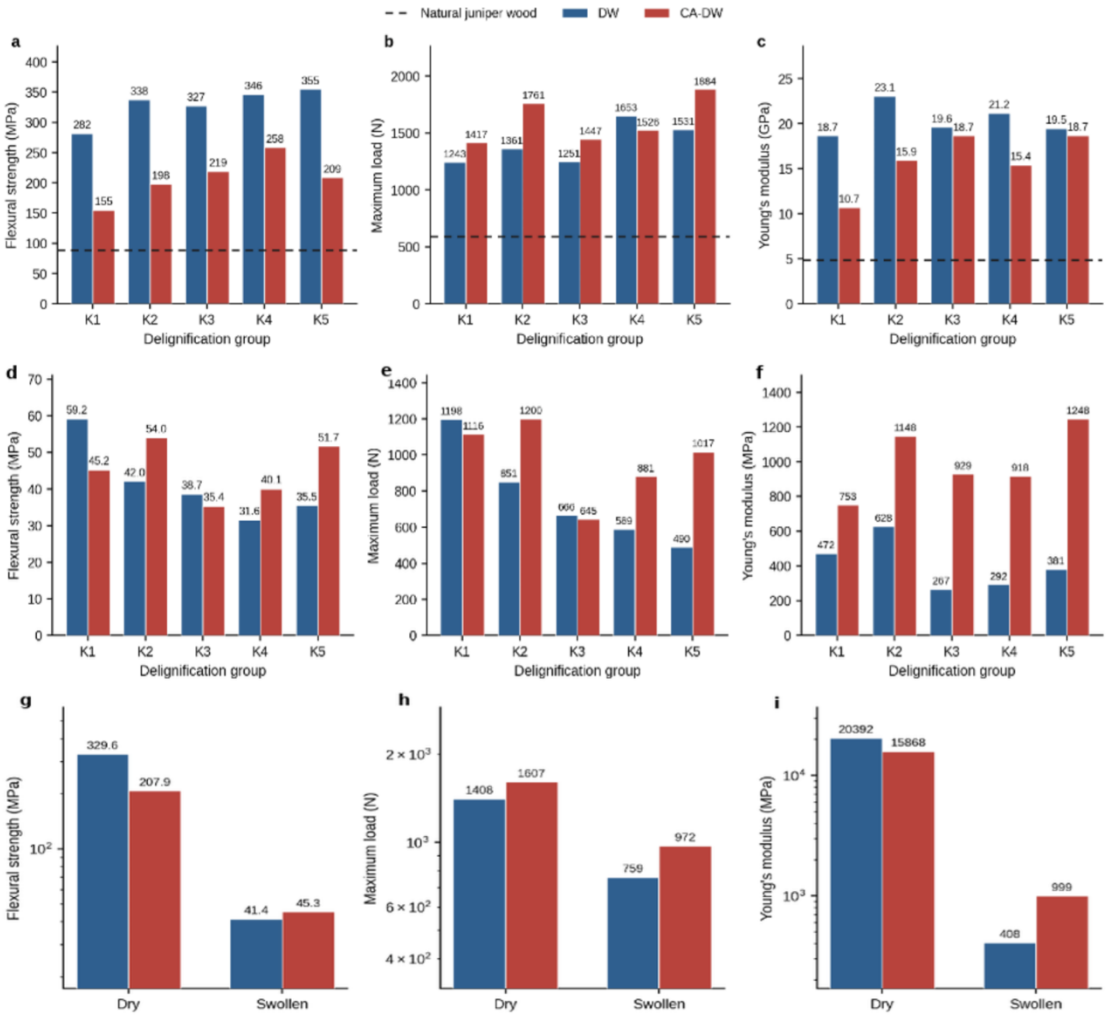


***Figure 17**: Mechanical properties of DW and CA-DW across delignification groups, in the dry and swollen states. (a–c) dry-state properties for each delignification group (K1–K5), with the dashed line marking the natural (untreated) juniper wood. (d–f) the same three properties measured after swelling in 0.9% saline at 37 °C, for the same delignification groups. (g–i) mean flexural strength, maximum load, and Young's modulus for DW and CA-DW pooled across all groups, plotted on a logarithmic y-axis.*

On the dry plates (a–c), DW and CA-DW show clear difference. Flexural strength is higher for DW in every K group (about 280–355 MPa against 155–258 MPa). Young's modulus follows that pattern as well in four groups (only K3 is close). That is the densification cost of citrate: the extra ester bonds in the wall resists collapse in the press more. So the dry CA-DW samples are weaker and usually less stiff when normalised by section size. However, for maximum load, CA-DW is higher: several CA-DW bars match or beat DW. Maximum load is only the force at break. Flexural strength and modulus divide that force by the bar's width and thickness, so they describe the material rather than that particular stick. CA-DW often stayed thicker in the press, so it can show a higher dry load and still a lower dry strength and modulus.

After swelling (d–f) the ranking flips for the properties that matter when wet. CA-DW flexural strength become slightly higher than DW (g) . Maximum load is generally higher for CA-DW once the plate is soaked, and Young's modulus is higher for CA-DW in every group. Water wrecks the hydrogen-bond network in DW, so the beam sags and modulus collapses. Ester holds in CA-DW cannot slide as far, so more of the dry stiffness survives and remains.

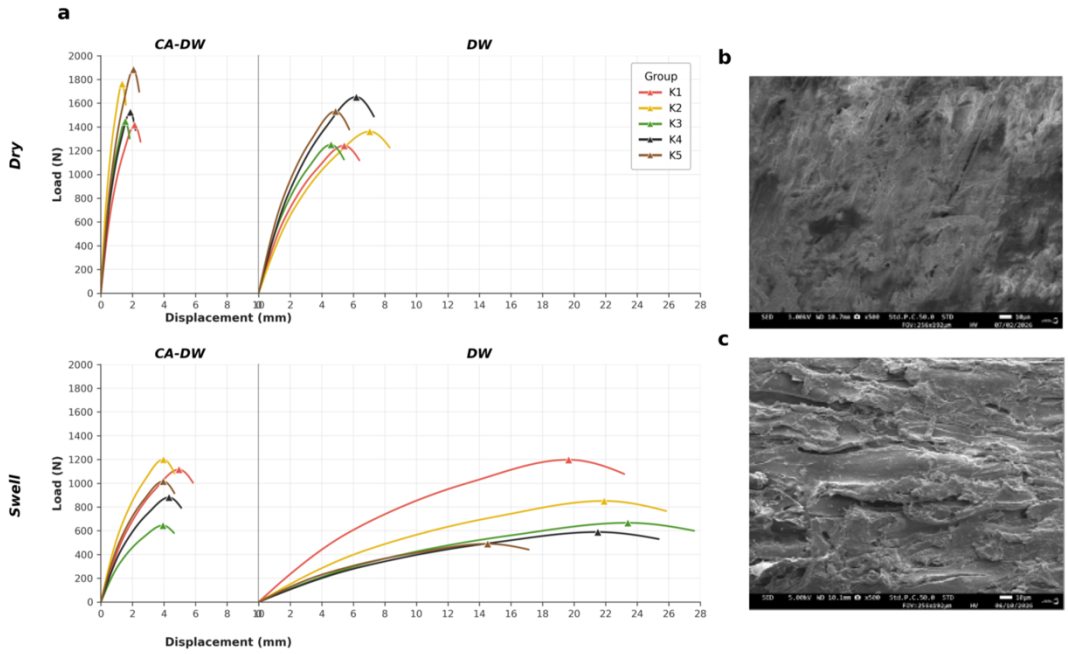


***Figure 18**: Mechanical performance and surface morphology of samples. a) Three-point bending load–displacement curves for CA-DW and DW across delignification groups K1–K5, in the dry and fully swollen states. b) SEM micrograph of a densified specimen surface at ×500 magnification (K5, dry) c) SEM micrograph of a separate densified specimen at ×500 magnification (K5, dry).*

Dry CA-DW curves rise almost vertically and drop before 2 mm of travel. Dry DW needs about 4–8 mm to reach the peak. After swelling that gap widens. CA-DW still peaks near 2–4 mm; DW runs out to 14–24 mm. Displacement at peak is how far the sample sagged before the load fell. A short stroke means the outer fibre reached failure strain while the bar had barely bent, which is more a stiff, brittle response. A long stroke means the network could keep deforming while not going complete break. Water turns DW even more ductile: the water softens the fibers and increases number of hydrogen bonds. Meanwhile, citrate esters, although stronger than single hydrogen bonds, its connection to fibers are less densified. Although the wet CA-DW peak has slightly higher displacement, its change is almost negligable compared to DW samples. This is because the OH sites of cellulsoe are already consumed by crosslinkage, and even if it is swelled, the numebr of hydrogend bonds avaliable with OH sites are little.

Figure b and c match that dry brittleness on the surface. The DW surface (b) is compacted and relatively smooth after the press. The CA-DW face (c), however, is stepped and cracked on surface, with open

layers rather than a closed skin. The 170 °C acid cure plus shrinkage of the citrate phase can open those flaws before the bending test starts. A bar that already carries surface cracks will fail at small displacement, which is exactly what dry CA-DW curves showed.

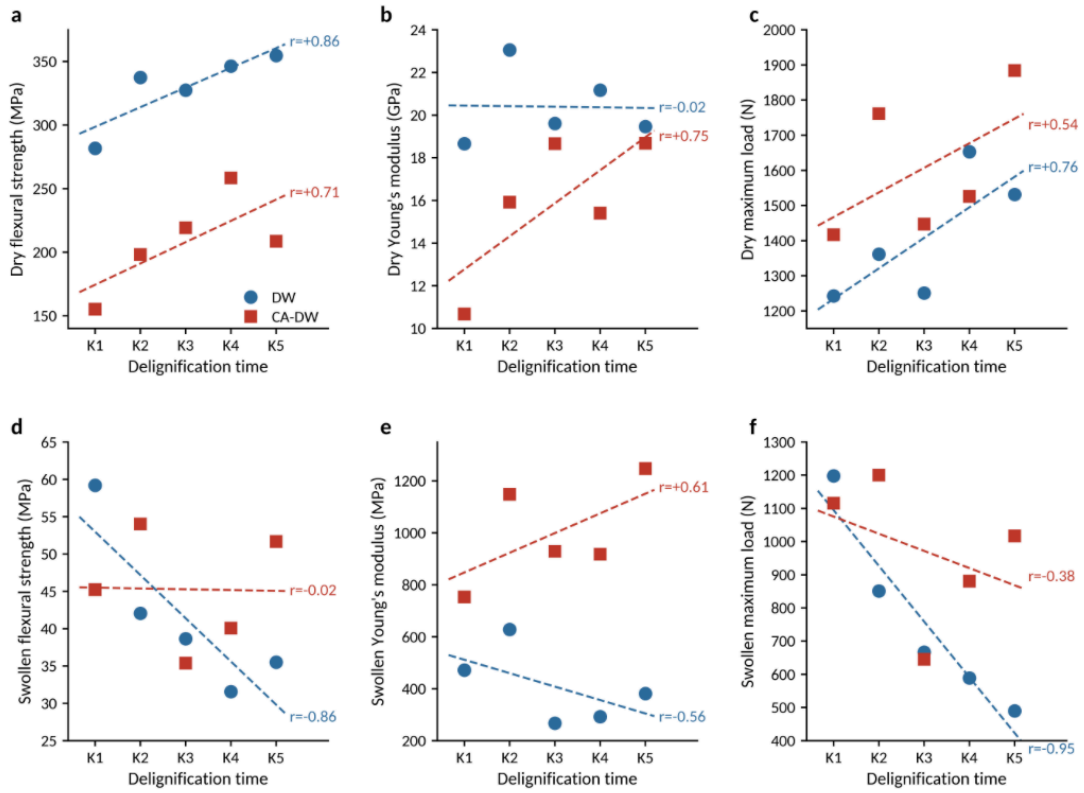


Figure 19: *Effect of delignification on the mechanical properties of DW and CA-DW in the dry and swollen states. (a) Dry flexural strength and (d) swollen flexural strength vs delignification time (groups K1–K5). (b) Dry Young's modulus and (e) swollen Young's modulus vs delignification time. (c) Dry maximum load and (f) swollen maximum load vs delignification time. Blue circles, uncrosslinked delignified wood (DW); red squares, citric acid-crosslinked delignified wood (CA-DW).*

Mechanical properties are correlated with cooking time. When dry, longer cooking goes with higher flexural strength for both materials (a: DW r = +0.86, CA-DW r = +0.71). That is the densification effect: more hours in alkali strip lignin and hemicellulose, the wall collapses further in the press, and the dry samples gets stronger. Dry modulus does not follow that trend. Against time (b), DW is flat (r = -0.02); CA-DW still rises (r = +0.75). Dry load rises with longer cooking for both materials (DW r = +0.76, CA-DW r = +0.54). Extra hours in alkali strip more structure, the strip packs harder under the press.

After swelling the signs change, and they change differently for the two materials. DW wet flexural strength falls hard with cooking time (d: r = -0.86): a more opened, lignin-poor plate takes more water and loses bending strength. CA-DW wet strength is flat against time (r = -0.02). The ester network, not the extra hour of cook, is what stabalizes the wet strength. Wet modulus (e) still drops with time for DW (r = -0.56) and rises for CA-DW (r = +0.61). A longer cook may leave more space for citric

acid to penetrate and crosslink, so the wet CA-DW plate keeps more stiffness; the same cook leaves DW more exposed to water. The sign flips for max load when samples are wet. Wet load falls with cooking time, steeply for DW (r = -0.95) and weakly for CA-DW (r = -0.38). A longer cook leaves a more opened, lignin-poor wall that takes more water and cannot carry force once the hydrogen bonds are gone. Ester bonds make the wood resist that drop a little, which is why the CA-DW line is flatter. Wet force here follows how badly the cook opened the plate, not how well it densified when dry.

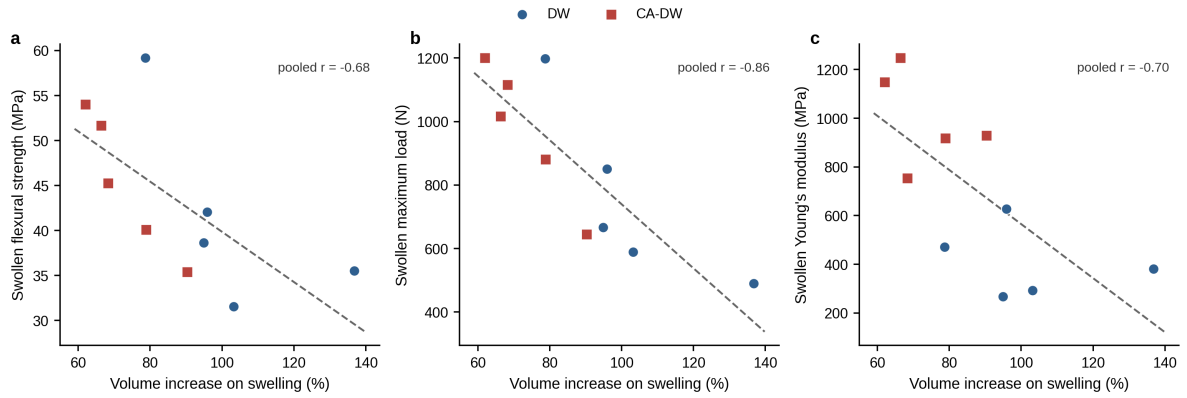


Figure 20: *Swollen mechanical properties as a function of the degree of swelling: (a) flexural strength, (b) maximum load, (c) Young's modulus, each plotted against the volume increase of the same specimen. Dashed lines are least-squares fits through the pooled data of both groups.*

The dimensional changes and mechanical datasets can also be directly cross-correlated. When each wet-state mechanical property is plotted against the volumetric swelling measured on the same specimen, a strong negative correlation emerges across the scattered data points for both groups, with correlation coefficients ranging from −0.68 to −0.86 (Figure 20). Specimens with lower water uptake retain a greater proportion of their mechanical performance. This finding supports a targeted interpretation of the crosslinking effect by proving that the enhanced wet-state performance of CA-DW arises from its reduced water absorption.

4.5 Degradability of densified wood

Densified wood consists predominantly of crystalline cellulose, and the human body does not secrete cellulase; as such, the material cannot be degraded to glucose *in vivo* at any physiologically relevant rate. Published implantation studies provide direct confirmation by showing that bulk cellulose meshes remain structurally intact and retrievable 90 days after implantation in rats, and nanofibrillated cellulose remains detectable via imaging 12 months post-injection in dogs [1,2]. Subcutaneously implanted plant-derived cellulose scaffolds similarly persist *in vivo* while maintaining good biocompatibility [11].

Across this body of literature, fragment size consistently emerges as the key determinant of *in vivo* fate. Cellulose clearance proceeds not via depolymerization, but via fragmentation followed by macrophage phagocytosis; accordingly, nanoscale and low-crystallinity cellulose forms that undergo ready

fragmentation are the forms observed to be fully cleared [1,3]. Fragmentation is therefore the rate-limiting step in physiological cellulose clearance, and the most meaningful metric to quantify is the mass of cellulose released from a specimen into its surrounding environment.

The present assay was designed around this principle. Specimens were fully immersed in simulated body fluid at 37 °C for 10 days in sealed vessels containing approximately 55 mL of free liquid volume. Cellulase was subsequently added to a 10.0 mL aliquot of the recovered liquid, not to mimic physiological processes, but purely as an analytical reagent to convert the released cellulose into glucose for colorimetric quantification.

Glucose concentration was quantified via the 3,5-dinitrosalicylic acid assay at 540 nm [12], calibrated against a five-point standard curve ranging from 0.1 to 0.5 mg mL^{-1} ($A = 3.453c + 0.440$, $R^2 = 0.9843$; Figure 21a). All sample absorbance values fell within the calibrated range, so all concentrations were derived by interpolation. Measured glucose concentrations were converted back to equivalent cellulose mass using the molar mass ratio of the anhydroglucose repeating unit to glucose (162.14/180.16 = 0.900), which corrects for the water molecule incorporated upon cleavage of each glycosidic bond.

Untreated juniper wood released 0.108 mg mL^{-1} of cellulose, DW samples released 0.250 mg mL^{-1}, and CA-DW samples released 0.375 mg mL^{-1} (Figure 21b, c). Densification alone therefore increased cellulose release relative to untreated wood. This trend is explained by the delignification step, which removes the hydrophobic lignin that normally shields cellulose in native wood; the densified material is thus physically more compact, but chemically more exposed to aqueous environments. Crosslinking further increased release by 49.6%, reaching 3.5 times the level measured in untreated samples, and this enhancement was consistently observed across all five delignification levels without exception.

This result is counterintuitive and represents the core finding of this study. CA-DW absorbs 29.4% less water than DW; by any conventional model in which degradation is driven by water ingress, CA-DW would therefore be expected to degrade more slowly. Instead, it degrades faster. Cellulose release is evidently governed not by the total volume of water penetrating the material, but by the presence of hydrolytically labile bonds within the material structure. The ester bridges introduced by citric acid modification undergo hydrolysis under mild aqueous conditions, whereas the β-1,4-glycosidic backbone of cellulose remains stable under physiological pH and temperature. Upon cleavage of an ester bridge, the cellulose chain it anchored is released from the polymer matrix.

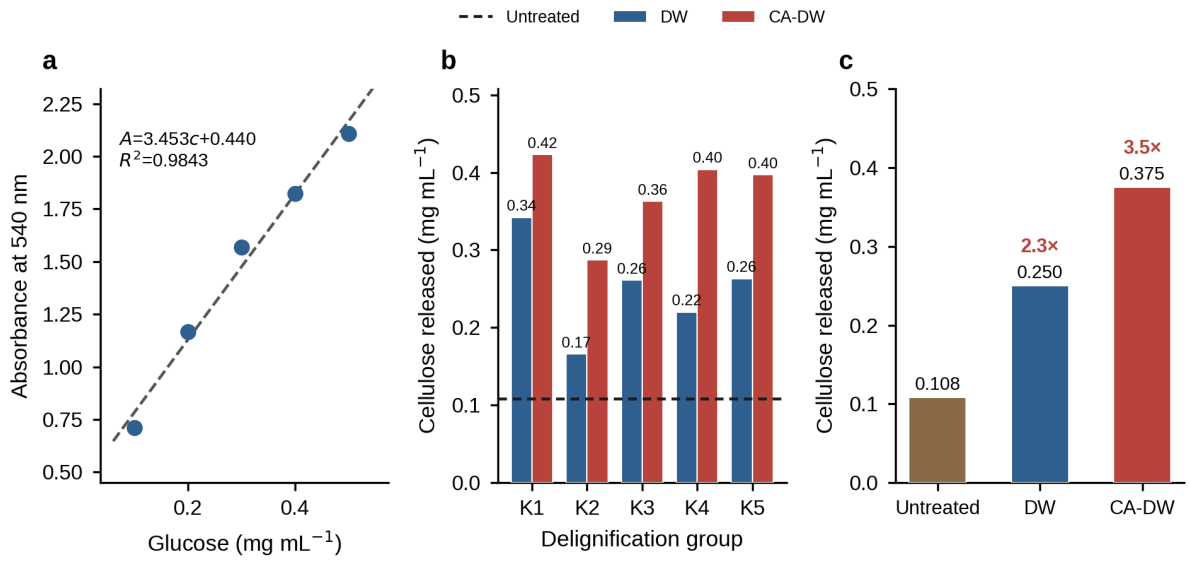


Figure 21: *Degradation in simulated body fluid. (a) Glucose calibration curve at 540 nm. (b) Cellulose released by each delignification group, untreated juniper dashed. (c) Group means; densification raises release 2.3-fold and crosslinking 3.5-fold.*

4.6 Impact of lignin and citric acid content

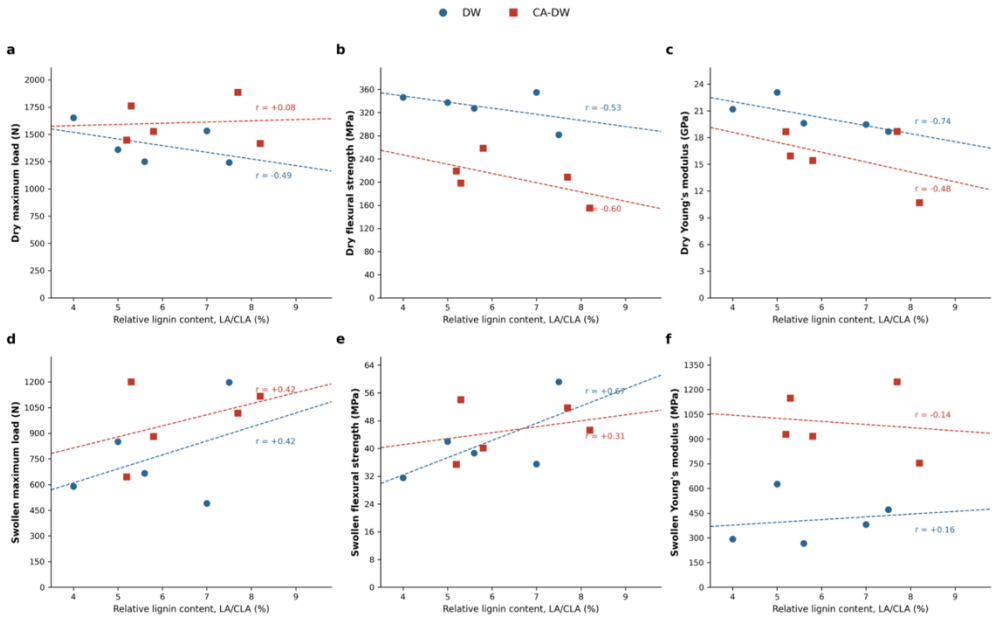


Figure 22*: Residual lignin versus dry and swollen bending properties of DW and CA-DW. a) Dry maximum load. b) Dry flexural strength. c) Dry Young's modulus. d) Swollen maximum load. e) Swollen flexural strength. f) Swollen Young's modulus. Blue, DW; red, CA-DW.*

Dry panels a–c belongs to one argument. Leftover lignin can work against densification. Dry flexural strength and dry modulus both fall as LA/CLA rises, for DW and for CA-DW. More lignin in the wall means less aligned cellulose–cellulose contact after the same press, so the dry solid is weaker and less stiff. Dry maximum load does not follow as cleanly, because load still includes thickness and width. A

CA-DW strip that did not crush as thin can keep a high force and still lose on MPa and GPa. Across a–c, CA-DW sits below DW on the size-normalized properties (strength, modulus) at a given lignin level: citrate resists the press and the acid–heat cure adds a dry penalty. Load can look similar or even higher for CA-DW for the geometry reason above.

Once the plates are wet, the ranking is no longer about who packed better. Swollen load and swollen strength turn up with lignin, clearly for DW and weaker for CA-DW. Residual lignin is hydrophobic and holds some contacts after hydrogen bonds fail, so a higher LA piece still carries a little more wet force. CA-DW is flatter on wet strength because the ester rungs already supply that constraint.

Swollen Young's modulus is the panel that actually separates the two networks. It barely tracks lignin at all (near-zero r for both series), yet CA-DW lies well above DW across the whole LA/CLA range. Wet stiffness is not a lignin dose. It is whether the sheet can open. DW is held by hydrogen bonds; water replaces those bonds and modulus collapses to a few hundred megapascals. CA-DW still has covalent tethers, so the wet beam cannot sag in the same way and modulus stays near 1 GPa. Lignin can nudge wet load and wet strength; it does not set wet modulus. The esters do.

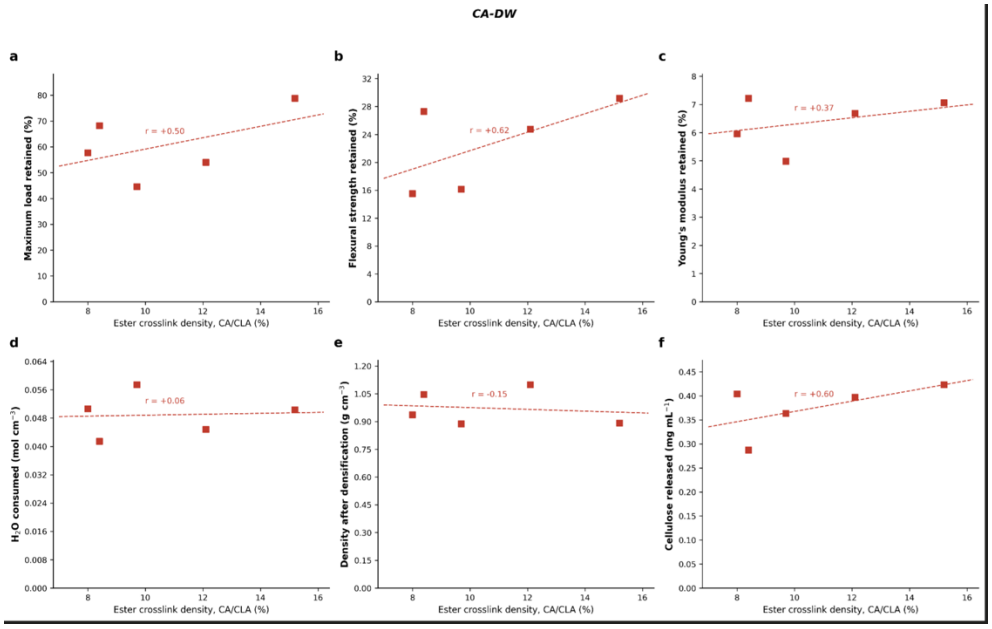


Figure 23: *CA/CLA ratio and wet retention and fragment release in CA-DW. a) Maximum-load retained after swelling (wet/dry). b) Flexural-strength retained. c) Young's-modulus retained. d) mole of water consumed per unit volume. e) Density after densification. f) Reducing-sugar released in the degradation assay.*

From Figure 23, it is clear that higher CA/CLA goes with higher retained load (r = +0.50), retained flexural strength (r = +0.62), and retained modulus (r = +0.37). This is a clear evidence that more ester signal means more covalent tethers after the hydrogen-bond network is flooded, so a larger fraction of the dry value survives.

Water uptake is flat (r = +0.06). Density after the press is flat to slightly down (r = -0.15). In this window extra esters do not show up as half the water or a denser board. Most OH remain free, and citrate in the wall can resist compaction, which cancels some anti-swell benefit. Retention can still rise if the water that does enter cannot push fibrils apart.

Cellulose released in the degradation assay rises with CA/CLA (r = +0.60). The same esters that hold the wet plate can hydrolyse in SBF and release cellulose more for the sugar measurement. So, the trend of high CA content means higher degradabiliity is clear.

4.7 Comparison with bone and established implant alloys

Given that this material was developed for fracture fixation applications, its key mechanical properties are benchmarked against those of cortical bone and three metallic alloys currently in clinical use (Figure 8). Stiffness represents the most favourable point of comparison. Cortical bone exhibits a Young's modulus of approximately 15–25 GPa [7]. By comparison, Ti–6Al–4V has a modulus of ~110 GPa, 316L stainless steel ~190 GPa, and cobalt–chromium alloy ~235 GPa, meaning these metallic implants are 5 to 12 times stiffer than the host tissue they are intended to support. With moduli of 20.4 GPa (DW) and 15.9 GPa (CA-DW), both materials fall squarely within the cortical bone modulus range (Figure 9). This is achieved at densities of only 0.97–1.13 g cm^{-3}, compared with 4.4–8.4 g cm^{-3} for the metallic alloys. In terms of specific strength, defined as flexural strength divided by density, DW achieves 291 MPa·cm^3·g^{-1}, which exceeds the value of approximately 211 MPa·cm^3·g^{-1} for titanium alloy.

All preceding comparisons correspond to dry-state properties. Under saturated conditions, the modulus of both materials drops to approximately 0.4–1.0 GPa, one to two orders of magnitude below the clinical requirement. This represents the primary limitation for clinical translation, and potential strategies to address this gap are discussed in Section 6.2.

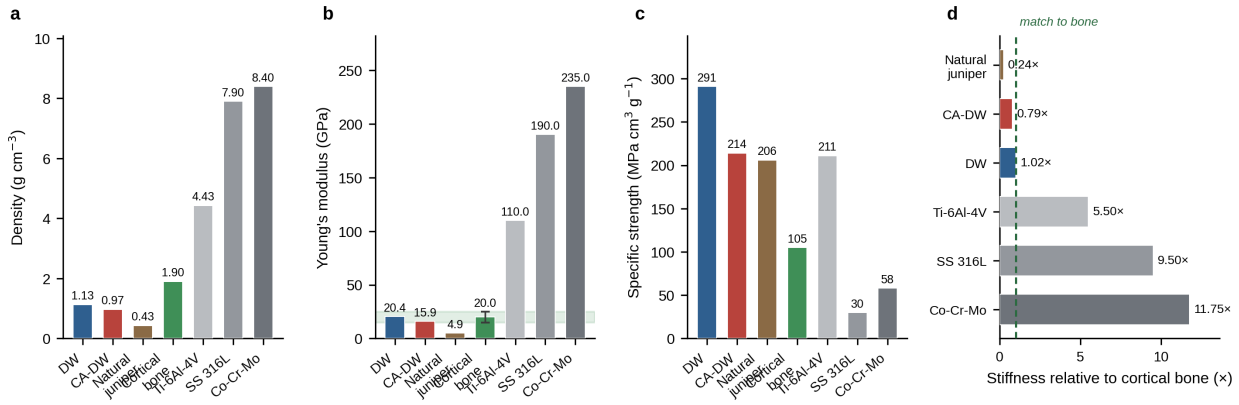


Figure 24: *Densified wood benchmarked against cortical bone and clinical implant alloys. (a) Density. (b) Young's modulus, with the cortical bone range shaded; error bars span reported literature values. (c) Specific strength, flexural strength divided by density. (d) Stiffness of each material as a multiple of the cortical bone median of 20 GPa; the dashed line marks an exact match.*

4.8 Measurement uncertainty

Each reported mechanical property value represents the mean across the five delignification groups, while each degradation absorbance measurement is the average of three replicate readings. Inter-group variability across delignification levels, expressed as the coefficient of variation, is summarised in Table 5. Two distinct trends are observable. First, data dispersion is consistently greater in the swollen state than in the dry state for both materials. This is expected since saturated, softened specimens are more sensitive to minor variations in sample geometry and water content. Second, CA-DW exhibits higher variability in the dry state but lower variability in the swollen state relative to DW. This is consistent with crosslinking conferring a more uniform response to water uptake, even as it introduces some heterogeneity in the degree of reaction across the material.

Table 5: *Coefficient of variation across the five delignification groups.*

Measurement	DW (%)	CA-DW (%)
Flexural strength, dry	8.7	17.9
Maximum load, dry	12.8	12.8
Young's modulus, dry	8.6	20.6
Flexural strength, swollen	25.8	17.2
Maximum load, swollen	36.7	22.4
Young's modulus, swollen	36.0	19.8
Volume increase on swelling	21.1	15.6
Mass uptake on swelling	21.4	21.0

4.9 Summary of the effect of crosslinking

Table 6 summarizes the key experimental measurements, and Figure 25 presents the percentage change in each measured property induced by crosslinking. Properties are ranked by magnitude of change and color-coded according to whether the change improves performance under wet service conditions. Of the fourteen properties quantified, eleven show improvement while three exhibit reduction.

The three reduced properties are dry flexural strength, dry modulus, and degree of densification, all of which stem from the same underlying mechanism: a cell wall stiffened prior to pressing undergoes less compaction. The eleven improved properties encompass all swollen-state characteristics, all metrics of dimensional stability, dry peak load, and cellulose release rate. Performance losses are confined exclusively to the dry state, while gains are fully concentrated in wet-state performance and degradability.

Table 6: *Summary of key properties. Values are means of the five delignification groups.*

Property	Untreated juniper	DW	CA-DW	Change on crosslinking
Dry flexural strength (MPa)	88.9	329.6	207.9	−36.9%
Dry Young's modulus (GPa)	4.86	20.4	15.9	−22.2%
Dry density (g cm⁻³)	0.432	1.132	0.972	−14.1%
Swollen flexural strength (MPa)	—	41.4	45.3	+9.4%
Swollen Young's modulus (MPa)	—	408	999	+144.8%
Flexural strength retained (%)	—	12.6	21.8	+73.4%
Young's modulus retained (%)	—	2.0	6.3	+214.6%
Volume swelling (%)	—	101.9	73.2	−28.2%
Mass uptake (%)	—	130.4	92.0	−29.4%
Cellulose released (mg mL⁻¹)	0.108	0.250	0.375	+49.6%

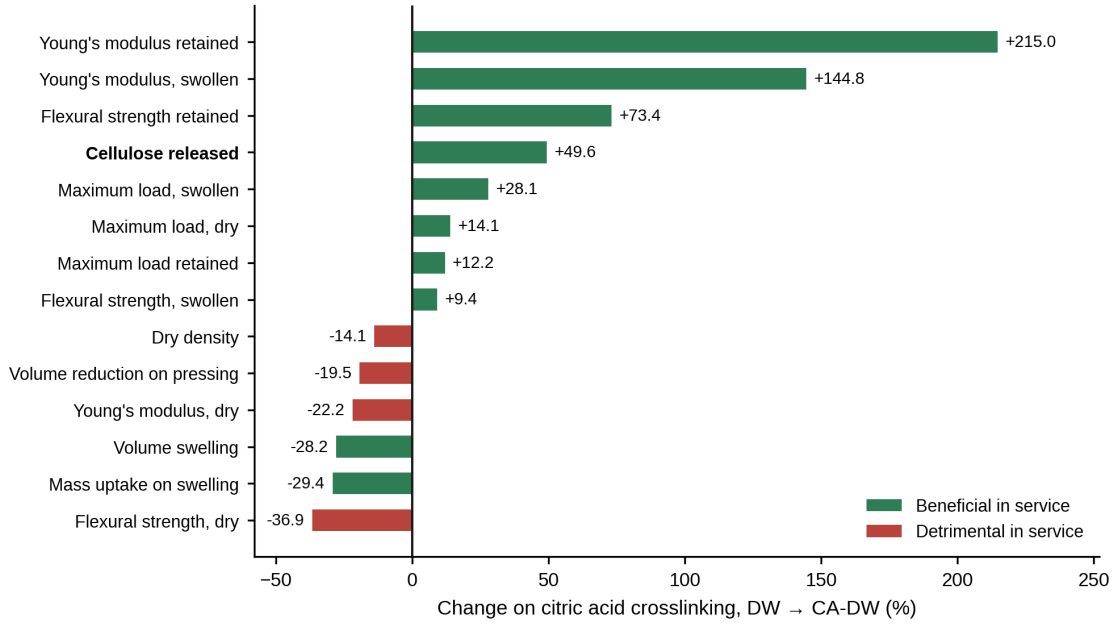


Figure 25: *Change in every measured property from DW to CA-DW, coloured by whether the change benefits performance in a wet service environment. For volume swelling and mass uptake a decrease is beneficial.*

5. Conclusions

Densified wood (DW) is strong, light, renewable and radiolucent, and its stiffness sits in the range of cortical bone, but the fact that it swells and loses most of its stiffness when wet have kept it out of any application as an implant involving water. It also degrades negligibly in simulated body fluid. This project asked whether replacing part of that interface with covalent but hydrolysable ester crosslinks would address these issues, and treated the mechanical and the degradation questions as two separate aspects of the same chemical change.

Chemically, the modification worked. Impregnating partially delignified juniper with 10 wt% citric acid and curing it before pressing produced ester crosslinks through the bulk of the material, confirmed by an infrared carbonyl band at 1715 to 1745 cm^{-1} that is absent from the uncrosslinked control, with matched lignin-to-cellulose ratios in both groups showing that crosslinking was the only variable between them.

On the mechanical aspect, every water-related property trended in the intended direction. Volume swelling fell by 28.2%, water uptake by 29.4%, retained stiffness after saturation rose 2.4-fold and retained flexural strength rose from 12.6% to 21.8% of the dry value. The direction of the hypothesis is therefore confirmed. The magnitude is not sufficient. Saturated stiffness is still close to 1 GPa against the 15 to 25 GPa of cortical bone, so the swelling problem that disqualifies densified wood has been reduced rather than solved, and the material as made here could not carry load as an implant in a wet environment. The interfacial energy analysis of Section 2.2 predicted a far larger effect, and the gap between that prediction and the measurement is itself a finding: the crosslink network formed is evidently less complete than the model assumed. Dry flexural strength also fell by 36.9%, which was not anticipated and is attributed to the stiffened cell wall resisting densification, an interpretation supported by the smaller volume reduction and lower density of the crosslinked specimens.

Dispite the reduction of performance in dry state, crosslinking still provides very meaning trends toward the rentention of the mechanical properties. In Section 4.6, for all mechanical properties measured, its rentention percentage showed clear positive correlation with CA/CLA, proving that citric acid crosslinkage can be use as a tool to improve rentention of physical properties in wood material under wet condition.

On the degradation aspect, cellulose release into simulated body fluid rose by 49.6% and did so at every delignification level. This is an original result, since the rate at which densified wood sheds cellulose has not previously been measured, and it establishes that the ester bridges provide a cleavage route the untreated material does not have. However, this finding does not establish resorption inside the human body due to the fact that humans secrete no cellulase, so released cellulose cannot be metabolised as a polyester implant is, and the fragments released here are larger than the forms for which clearance from tissue has been demonstrated. The goal of a material that disappears after healing therefore remains unmet.

The honest overall conclusion is that citric acid crosslinking of densified wood works, in the sense that both intended effects were produced and measured, but not yet to a degree that makes the material usable as a bone implant. What the project contributes is the demonstration that this route exists and is chemically

represented, together with a quantified account of how far it goes and why it stops there. The approach is original to this work and none of its parameters have been optimised; pressing pressure, citric acid concentration and cure conditions were each fixed at a single value in the current investigation, and the results give clear reasons to expect that varying them would improve the outcome. Bone fixation was the problem that prompted the investigation, but the transferable result is the crosslinking approach and the finding that swelling resistance and degradability can be improved.

6. Discussion

6.1 Mechanical performance

The hypothesis set out in Section 2 was that converting part of a hydrogen-bonded interface into covalent ester crosslinks would reduce swelling and preserve mechanical properties in water. Every relevant measurement moved in the predicted direction, and the effect was consistent showing how crosslinked specimens swelled less, absorbed less water and retained more of their dry stiffness and strength at every one of the five delignification levels. The correlation between the degree of swelling and the retained properties across both groups, supports the proposed mechanism directly, since specimens that took up less water retained more performance regardless of which group they belonged to.

The size of the effect is another matter. A water saturated modulus near 1 GPa is significantly below what a load-bearing fixation plate requires. Crosslinking narrowed the gap between the dry and wet states without coming close to closing it, thus, the central weakness of densified wood which is losing its mechanical identity in water, remains unsolved after the treatment. Therefore, the material produced in this investigation remains not usable as an implant, and the barrier identified in Section 1.3 remains open.

The theoretical analysis and the experiment diverge, and the divergence is informative in a scientific context. The calculation in Section 2.2 treated the crosslinked interface as though every modelled ester formed and contributed its full bond energy, and on that basis predicted an interface several times stronger than the hydrogen-bonded sample. However, the promising yet limiting effects on swelling and physical property retention in wet state infers that the crosslink network is considerably less complete than the model assumed. Citric acid must diffuse into a cell wall and find hydroxyl groups that are sterically accessible, and only a fraction of the sites counted in the model are likely to meet that condition; the infrared ester-to-cellulose ratios, which was between 8 and 15%, are consistent with partial rather than extensive substitution. The hydrogen-bond substitution was therefore overestimated in the sense that too much of it was assumed to have been replaced.

A second result ran against expectation. Dry flexural strength fell by 36.9% and dry stiffness by 22.2%. This decrease could be explained in a mechanical context and the evidence for it is in the densification

data. Crosslinks formed before pressing stiffen the cell wall, so the same 5 Mpa, 24h pressing produces less densification showed by the crosslinked specimens having a volume reduction of 52.1% against 64.7% for the uncross linked densified wood, and a dry density of 0.97 against 1.13 g cm^{-3}. A less compacted material has fewer load-bearing contacts per unit area, and the loss of those contacts outweighs the strength of the individual bridges that replaced them.

Set against this, the result remains successful rather than a failure. The chemistry does what it was designed to do, the effects are measurable and reproducible across five processing conditions, and no parameter has yet been optimised. Pressing pressure, citric acid concentration and method of treatment were each held at one value throughout the investigation, which has room to better experimental variable in a favourable direction for crosslinked samples. The coating route described in Section 6.2 also remains available and is independent of any further gain from crosslinking. *What this work establishes is that the path is real and worth following, not that it has been followed to its end.*

6.2 Degradability

Degradability was pursued as a separate objective. The reason a resorbable plate is wanted at all is to avoid the second operation described in Section 1.1, and the barrier identified in Section 1.3 was that densified wood sheds essentially no material in water because the accessible bonds are hydrogen bonds and the inaccessible ones are glycosidic. The prediction was that ester bridges would provide cleavable junctions.

That prediction was confirmed by the result. Crosslinked specimens released 49.6% more cellulose into simulated body fluid than the control, and 3.5 times as much as untreated juniper, with the increase appearing at every delignification level. It is worth mentioning that the direction of the result is the opposite of what a simple water-transport argument would predict, since the crosslinked material absorbs 29.4% less water yet releases half as much cellulose, which shows that release is governed by the population of hydrolysable bonds rather than by how much water enters the sample.

What the result does not show is that the material degrades in the body. As previously mentioned, since humans secrete no cellulase, cellulose released from the material cannot be metabolised to glucose. No route for clearing fibre-scale cellulose from tissue has been established, thus, the objective of a plate that disappears after union is not met by this work. However, the increased fibre release is still a necessary step towards resorption, since detachment is the first step towards resorption.

Several routes might close that gap, however they could not be tested in the current investigation. Cellulase could in principle be co-delivered locally from the same coating that protects the core during healing. Cellulose crystallinity could be reduced during processing so that the fragments released are small enough for phagocytic clearance. Alternatively the material could be directed at applications in which a slowly encapsulated residue is acceptable, or at uses outside the body where degradability is

needed but human metabolism is irrelevant. The measurement made here is what makes any of these testable, since it provides a way of quantifying release that did not previously exist.

6.3 Materials-science contribution

Citric acid esterification is a part of chemistry that is pre-established. During heating, two adjacent carboxyl groups dehydrate to a cyclic anhydride, which a hydroxyl group opens to give an ester and regenerate a carboxyl that can react again, so one tricarboxylic molecule can bridge several chains [18,19]. But what has not been established nor proven is whether that theory can be made to work on a bulk lignocellulosic solid.

Previous studies of citric acid crosslinking have been carried out almost entirely on isolated or reconstituted cellulose such as purified fibres, wood powder bound with a cellulose derivative, films and hydrogels [18,19]. These are systems in which every chain is already accessible to the reagent. Wood is a completely different system. It is a hierarchical composite in which crystalline cellulose microfibrils are embedded in hemicellulose and encased in hydrophobic lignin, and the reagent must reach sites buried inside a cell wall rather than dispersed in suspension. Whether a crosslink network would be formed in such complex, and what it would do to properties that depend on the composite architecture rather than on individual chains, could not be predicted from any earlier work. Establishing that it does form, and quantifying what it changes, is the first contribution of this study.

The second lies in where the step was placed. Delignification opens the cell wall and exposes hydroxyl groups, so carrying out the crosslinking after that step but before pressing puts the reagent into an open structure that is then closed around it. Reversing the order would confine the reaction to the surface, because a densified specimen can no longer be impregnated internally. The choice was proven to cause a fifth of the achievable densification to be reduced and was made deliberately for that reason, which is why it would not be reached by following the conventional logic of maximising density.

The third contribution is the one most likely to transfer. Dimensional stability and degradability are usually treated separately, on the reasoning that whatever keeps water out also slows hydrolysis. The result in this investigation shows that swelling is governed by the availability of free hydroxyl groups, while degradation by the presence of bonds that water can cleave, and a polycarboxylic acid alters both at once in opposite directions. Nothing in that argument is specific to citric acid or to juniper, and it should apply to other polycarboxylic crosslinkers and other hydroxyl-rich biopolymers.

Lastly, the postive correlation of physical property rentention when swelled with citric acid crosslinkage is worth noting. This clear positive correlation throughout all mechancial properties provides a way to improve retention of mechanical properties when swelled in the field of wood science.

6.4 Recommended further investigation

The most immediate priority is pressing pressure. The dry-strength loss reported in Section 6.1 is attributed to a stiffened cell wall compacting less at a fixed 5 Mpa which is the pressure inherited from work on uncrosslinked wood. Pressing crosslinked specimens at higher pressures, while measuring the change in density, volume reduction and strength, would test that explanation directly and may recover most of the dry properties that were lost. *Since the crosslinked material is furthest from its attainable density, it has the most to gain.*

A citric acid concentration series should follow, extending in both directions from the single value of 10 wt% used in this investigation. Higher concentrations would raise crosslink density and test whether the wet-state retention can be pushed towards a useful level. Lower concentrations would establish whether most of the benefit remains at a smaller decrease in dry strength. Either way, a series of range is what is needed to fully explore the mechanism argued here, which is what a single concentration data cannot do.

Degradation should also be followed at several time points rather than one, with the released material sized, since fragment size determines whether phagocytic clearance is available at all. A blank containing cellulase but no specimen should be included as well, because enzyme preparations contribute a small quantity of reducing sugar to every reading. Testing whether cellulase can be co-delivered from a coating would also be valuable in terms of addressing the resorption limitation.

The protective coating concept requires experimental validation. A resorbable hydrophobic barrier such as poly(L-lactic acid), whose degradation period is tunable through molecular weight, crystallinity and coating thickness [15], would exclude fluid during the three to six months in which a fracture regains most of its strength and then break down, admitting water to the material that is by then no longer required to bear load and provide support. Crosslinking is what would make that second stage proceed at a useful rate. This route addresses the wet-state weakness from a different direction than crosslinking does, and the two are complementary to each other.

Biological testing could be worth including in order to practically verify the biocompatibility of the material. Juniper was chosen partly because its essential oils are antiseptic and because untreated juniper implanted in rabbits was tolerated for up to three years with bone growing into the wood [8,16,17], so the starting material is promising. However, delignification and crosslinking change the surface of the samples substantially, and cytotoxicity, immune response and in vivo behaviour of the modified material are untested, thus, whether the treated material remains biocompatible is questionable.

7. References

[1] Morgan, E. F., Unnikrisnan, G. U. & Hussein, A. I. Bone mechanical properties in healthy and diseased states. Annual Review of Biomedical Engineering 20, 119–143 (2018).

[2] Rijs, Z. et al. Metal artefact reduction in orthopaedic imaging. Scientific Reports 14 (2024).

[3] Lam, F. C. et al. Carbon-fibre-reinforced PEEK implants and imaging compatibility. Brain Sciences 15, 199 (2025).

[4] Rabin, B. Orthopaedic implant materials: stainless steel 316L composition and nickel sensitivity. Medscape Reference (2024).

[5] Märtson, A. et al. Biocompatibility of cellulose material in bone tissue (1999).

[6] Song, J. et al. Processing bulk natural wood into a high-performance structural material. Nature 554, 224–228 (2018).

[7] NileRed. Making wood as strong as steel. YouTube (2024). https://www.youtube.com/watch?v=CglNRNrMFGM

[8] Andze, L. et al. Chemically pretreated densification of juniper wood for potential use in osteosynthesis bone implants. Journal of Functional Biomaterials 15, 287 (2024). https://www.mdpi.com/2079-4983/15/10/287

[9] Verma, D. Chemical structure of cellulose, hemicellulose and lignin. ResearchGate figure (2024). https://www.researchgate.net/figure/Chemical-structure-of-cellulose-hemicellulose-and-lignin_fig5_382914170

[10] Wei, J. et al. Citric acid crosslinking of polysaccharide systems. Food Hydrocolloids (2023). https://www.sciencedirect.com/science/article/abs/pii/S0268005X23006446

[11] Huang, Y. et al. Citric acid modification of lignocellulosic materials. Polymers 16, 1647 (2024). https://www.mdpi.com/2073-4360/16/12/1647

[12] Sharmin, E. et al. Citric acid as a crosslinking agent for cellulosic materials. Polymers 17, 2064 (2022). https://www.mdpi.com/2073-4360/17/15/2064

[13] Nishiyama, Y. Molecular interactions in nanocellulose assembly. Philosophical Transactions of the Royal Society A 376 (2018).

[14] Modulevsky, D. J., Cuerrier, C. M. & Pelling, A. E. Biocompatibility of subcutaneously implanted plant-derived cellulose biomaterials. PLOS ONE 11, e0157894 (2016).

[15] Middleton, J. C. & Tipton, A. J. Synthetic biodegradable polymers as orthopedic devices. Biomaterials 21, 2335–2346 (2000).

[16] Gross, K. A. & Ezerietis, E. Juniper wood as a possible implant material. Journal of Biomedical Materials Research Part A 64, 672–683 (2003). https://pubmed.ncbi.nlm.nih.gov/12601779/

[17] Nefjodovs, V. et al. Wood as possible renewable material for bone implants: literature review. Journal of Functional Biomaterials 14, 266 (2023). https://www.mdpi.com/2079-4983/14/5/266

[18] Tao, X. & Nonaka, H. Wet extrusion molding of wood powder with hydroxypropylmethyl cellulose and with citric acid as a crosslinking agent. BioResources 16, 2314–2325 (2021). https://bioresources.cnr.ncsu.edu/resources/wet-extrusion-molding-of-wood-powder-with-hydroxy-propylmethyl-cellulose-and-with-citric-acid-as-a-crosslinking-agent/

[19] Citric acid as a green modifier for wood: a review. Polymers 12, 1692 (2020).

[20] Gusakov, A. V. et al. Comparison of two methods for assaying reducing sugars. International Journal of Analytical Chemistry (2011). https://pmc.ncbi.nlm.nih.gov/articles/PMC3103847/

[21] Cellulase assays: standard protocols. Sigma-Aldrich technical document. https://www.sigmaaldrich.com/JM/en/technical-documents/protocol/protein-biology/enzyme-activity-assays/enzymatic-assay-of-cellulase

[22] Dashtban, M., Maki, M., Leung, K. T., Mao, C. & Qin, W. Cellulase activities in biomass conversion: measurement methods and comparison. Critical Reviews in Biotechnology 30, 302–309 (2010). https://doi.org/10.3109/07388551.2010.490938

[23] Miller, G. L. Use of dinitrosalicylic acid reagent for determination of reducing sugar. Analytical Chemistry 31, 426–428 (1959). https://pubs.acs.org/doi/10.1021/ac60147a030

[24] Comparative in vivo biocompatibility of cellulose-derived and synthetic meshes in subcutaneous transplantation models. Biomacromolecules 25 (2024). https://pubs.acs.org/doi/10.1021/acs.biomac.4c00984

[25] In vivo biocompatibility and long-term durability of nanofibrillated cellulose as a urethral bulking agent in rats and Beagle dogs. PLOS ONE 20 (2025).

[26] Longitudinal monitoring of nanofibrillar cellulose hydrogel medical implants using positron emission tomography. Journal of Controlled Release (2025).

[27] USDA Forest Service. Mechanical properties of juniper. Forest Products Laboratory. https://research.fs.usda.gov/treesearch/55957

[28] Wolff's Law and Bone Fracture Recovery. Respire Physical Therapy web article (2023). https://respirept.com/wolffs-law-and-bone-fracture-recovery/](https://respirept.com/wolffs-law-and-bone-fracture-recovery/

[29] Poly(lactic acid) degradation in the human body. ResearchGate figure. https://www.researchgate.net/figure/Polylactic-acid-PLA-degradation-in-the-human-body_fig6_319987351

[30] Poly(L-lactic acid), IV 5.0 dL/g. Polysciences product data. https://polysciences.com/products/poly-l-lactic-acid-iv-5-0-dl-g

[31] Embodied energy of common materials. Low-tech Magazine (2009). https://solar.lowtechmagazine.com/2009/06/how-much-energy-does-it-take-on-average-to-produce-1-kilogram-of-the-following-materials/

[32] Delignification of wood: optical images before and after treatment. ResearchGate figure. https://www.researchgate.net/figure/Delignification-of-wood-an-optical-image-of-original-wood-OW-before-a-and-after-b_fig1_330227703

9. Appendix

Table A1. Complete three-point bending data. Means are of the five delignification groups.

Material and property	State	K1	K2	K3	K4	K5	Mean
Untreated flexural strength (MPa)	Dry	—	—	—	—	—	88.90
DW flexural strength (MPa)	Dry	281.81	337.52	327.42	346.34	354.77	329.57
DW flexural strength (MPa)	Swollen	59.19	42.05	38.66	31.57	35.51	41.39
CA-DW flexural strength (MPa)	Dry	155.14	198.11	219.14	258.47	208.67	207.91
CA-DW flexural strength (MPa)	Swollen	45.24	54.02	35.38	40.08	51.67	45.28
DW maximum load (N)	Dry	1242.89	1361.39	1250.83	1652.72	1531.42	1407.85
DW maximum load (N)	Swollen	1197.71	850.92	666.44	589.20	489.89	758.83
CA-DW maximum load (N)	Dry	1416.60	1761.31	1447.13	1525.89	1884.25	1607.04
CA-DW maximum load (N)	Swollen	1115.71	1200.33	645.13	880.89	1016.74	971.76
DW Young's modulus (MPa)	Dry	18661.8	23054.0	19608.1	21171.5	19465.3	20392.1
DW Young's modulus (MPa)	Swollen	472.0	627.8	267.2	292.4	381.3	408.2
CA-DW Young's modulus (MPa)	Dry	10681.5	15921.5	18659.4	15402.6	18675.2	15868.1
CA-DW Young's modulus (MPa)	Swollen	753.5	1148.3	929.2	917.6	1247.7	999.3
DW displacement at failure (mm)	Dry	2.369	2.266	2.870	2.309	2.893	2.542
CA-DW displacement at failure (mm)	Dry	0.964	0.607	0.699	0.839	0.931	0.808

Table A2. Swelling, density and volume data.

Property	Group	K1	K2	K3	K4	K5	Mean
Volume increase (%)	DW	78.7	95.9	94.9	103.2	136.8	101.9
Volume increase (%)	CA-DW	68.3	62.0	90.3	78.9	66.4	73.2

Mass uptake (%)	DW	98.8	122.9	122.2	132.9	175.1	130.4
Mass uptake (%)	CA-DW	101.6	71.3	116.5	97.3	73.5	92.0
Dry density (g cm⁻³)	DW	1.118	1.204	1.227	0.996	1.116	1.132
Dry density (g cm⁻³)	CA-DW	0.892	1.045	0.887	0.937	1.099	0.972
Volume after pressing (cm³)	DW	7.27	6.10	5.40	6.16	5.17	6.02
Volume after pressing (cm³)	CA-DW	8.80	8.84	7.06	8.18	7.97	8.17
Volume reduction (%)	DW	57.4	64.2	68.3	63.8	69.6	64.7
Volume reduction (%)	CA-DW	48.3	48.1	58.6	52.0	53.2	52.1

Table A3. FTIR peak-area ratios, normalised to the cellulose C–O band at 1000–1100 cm⁻¹.

Group	DW LA/CLA (%)	CA-DW LA/CLA (%)	CA-DW CA/CLA (%)	Hemicellulose
K1	7.5	8.2	15.2	not detected
K2	5.0	5.3	8.4	not detected
K3	5.6	5.2	9.7	not detected
K4	4.0	5.8	8.0	not detected
K5	7.0	7.7	12.1	not detected

Table A4. Glucose calibration standards, absorbance at 540 nm (three trials each).

Glucose (mg mL⁻¹)	Trial 1	Trial 2	Trial 3	Mean
0.1	0.7082	0.7126	0.7102	0.7103
0.2	1.1602	1.1690	1.1702	1.1665
0.3	1.5634	1.5754	1.5698	1.5695
0.4	1.8226	1.8242	1.8234	1.8234
0.5	2.1066	2.1086	2.1106	2.1086

Table A5. Degradation assay: absorbance at 540 nm and derived cellulose release.

Group	Trial 1	Trial 2	Trial 3	Mean	Glucose (mg mL⁻¹)	Cellulose (mg mL⁻¹)
Untreated juniper	0.858	0.853	0.848	0.8530	0.1197	0.108
DW K1	1.745	1.754	1.754	1.7510	0.3797	0.342
DW K2	1.077	1.079	1.078	1.0780	0.1849	0.166
DW K3	1.450	1.434	1.444	1.4427	0.2904	0.261
DW K4	1.283	1.283	1.285	1.2837	0.2444	0.220
DW K5	1.443	1.448	1.453	1.4480	0.2920	0.263
DW Mean	—	—	—	—	**0.2783**	**0.250**
CA-DW K1	2.057	2.063	2.065	2.0617	0.4697	0.423
CA-DW K2	1.536	1.550	1.540	1.5420	0.3192	0.287
CA-DW K3	1.828	1.833	1.833	1.8313	0.4030	0.363
CA-DW K4	1.982	1.989	1.993	1.9880	0.4484	0.404
CA-DW K5	1.962	1.964	1.964	1.9633	0.4412	0.397
CA-DW Mean	—	—	—	—	**0.4163**	**0.375**

Table A6. Correlation coefficients between processing variables, composition and dry mechanical properties (n = 5 per series).

Relationship	DW	CA-DW
Flexural strength vs delignification time	+0.86	+0.71
Maximum load vs delignification time	+0.76	+0.54
Young's modulus vs delignification time	−0.02	+0.75
Flexural strength vs residual lignin	−0.53	−0.61
Young's modulus vs residual lignin	−0.74	−0.48
Swollen properties vs volume swelling (pooled)	−0.68 to −0.86	—